Najafi, Arsalan; Homaee, Omid; Jasiński, Michał; Pourakbari-Kasmaei, Mahdi; Lehtonen, Matti; Leonowicz, Zbigniew

Participation of hydrogen-rich energy hubs in day-ahead and regulation markets: A hybrid stochastic-robust model

Published in:
Applied Energy

DOI:
10.1016/j.apenergy.2023.120976

Published: 01/06/2023

Document Version
Peer-reviewed accepted author manuscript, also known as Final accepted manuscript or Post-print

Participation of Hydrogen-Rich Energy Hubs in Day-Ahead and Regulation Markets: A Hybrid Stochastic-Robust Model

Arsalan Najafi[a], Omid Homaee[a], Michał Jasiński[a,b,], Mahdi Pourakbari-Kasmaei[c], Matti Lehtonen[c], and Zbigniew Leonowicz[a,b]

[a] *Department of Electrical Engineering Fundamentals, Faculty of Electrical Engineering, Wroclaw University of Science and Technology, Wroclaw, Poland*
[b] *Department of Electrical Power Engineering, Faculty of Electrical Engineering and Computer Science, VSB-Technical University of Ostrava, 708-00 Ostrava, Czech Republic*
[c] *Department of Electrical Engineering and Automation, Aalto University, 02150, Maarintie 8, Espoo, Finland*

Abstract

Hydrogen-based technologies are one of the pathways toward a carbon-neutral world. This paper proposes a hybrid stochastic-robust framework for the optimal operation of hydrogen-based energy hubs (EHs) for a short-term horizon. The EH operator, as a large consumer, should make decisions to procure the required energy to meet the demands dealing with uncertainties in real-time. To manage the EH efficiently, the EH operator participates in the regulation market (RM) deploying regulation up (RU) and regulation down (RD) actions to compensate for the errors stem from the forecasting procedure in intra-hours. In addition, the EH should support the required hydrogen for hydrogen vehicles (HVs) on a hydrogen refueling station. Power-to-gas unit alongside a gas storage system links the electricity and natural gas network, and it facilitates the heat demand errors in intra-hours using gas-fed boilers. The uncertainty of the demands and the initial state of charge of the HVs are addressed by stochastic programming, while the uncertainty of the RM prices is considered by robust optimization to reach the worst-case realization of the RM prices. The simulation results demonstrate the effectiveness of the proposed framework in managing the hydrogen-rich EH

Email address: michal.jasinski@pwr.edu.pl Corresponding author (Michał Jasiński)

and energy storage systems with the day-ahead and real-time horizons. The amount of 14% error in electricity demands in the intra hours is resulted in 10% increases in purchasing from the RM at the same time.

Keywords: Energy hub, hydrogen, electrolyzer, hydrogen tank, CHP, power-to-gas technology, robust optimization, Hydrogen vehicle.

Nomenclature

A. Sets :

$\mathcal{T}$	Set of operating timeslots.
$\mathcal{T}_t$	Set of intra-hour operating timeslots.
$\mathcal{E}$	Set of electrolyzers.
$\mathcal{V}$	Set of hydrogen vehicles
$\mathcal{V}_t$	Set of hydrogen vehicles referring to the hydrogen refueling station at the tth operating timeslot.
$\mathcal{F}$	Set of fuel cells.
$\mathcal{H}$	Set of hydrogen tanks.
$\mathcal{G}$	Set of power-to-gas storage.
$\mathcal{B}$	Set of boilers.
$\mathcal{C}$	Set of combined heat and power systems.
$D_{\mathrm{DA}}, D_{\mathrm{RM}}$	Sets of decision variables.
§	Set of scenarios.

B. Indexes:

t	Index of operating timeslots.

j	Index of intera-hour operating timeslots.
e	Index of operating electrolyzers.
v	Index of hydrogen vehicles.
f	Index of fuel cells.
h	Index of hydrogen tanks.
g	Index of power-to-gas storage systems.
b	Index of boilers.
c	Index of combined heat and power systems.
s	Index of scenarios.

C. Parameters:

Mol^{H}	The molar mass of hydrogen.
$L^{\mathrm{HV,H}}$	Low heat value of hydrogen.
η_e^{Elz}	Efficiency of the eth electrolyzer.
$P_e^{\mathrm{Elz,Min}}$	Minimum power input of the eth electrolyzer.
$P_e^{\mathrm{Elz,Max}}$	Maximum power input of the eth electrolyzer.
$\kappa_e^{\mathrm{Elz,Max}}$	Maximum permissible increment in power input of the eth electrolyzer in two consecutive timeslots (in $\frac{kW}{h}$).
$\kappa_e^{\mathrm{Elz,Min}}$	Maximum permissible decrement in power input of the eth electrolyzer in two consecutive timeslots (in $\frac{kW}{h}$).
$\chi_{e,h}$	A binary variable that equals to 1 if the hydrogen produced by the eth electrolyzer is stored in the hth hydrogen tank.

$H_h^{\mathrm{PHT,Max}}$	Maximum permissible hydrogen pressure of the hth hydrogen tank.
$H_h^{\mathrm{PHT,Min}}$	Minimum permissible hydrogen pressure of the hth hydrogen tank.
V_h^{HT}	Volume of the hth hydrogen tank.
$T_{h,t}^{\mathrm{HT}}$	Temperature of hydrogen in the hth hydrogen tank.
$P_f^{\mathrm{FC,Min}}$	Minimum power output of the fth fuel cell.
$P_f^{\mathrm{FC,Max}}$	Maximum power output of the fth fuel cell.
$\kappa_f^{\mathrm{FC,Max}}$	Maximum permissible increment in input power of the fth fuel cell in two consecutive timeslots (in $\frac{kW}{h}$).
$\kappa_f^{\mathrm{FC,Min}}$	Maximum permissible decrement in input power of the fth fuel cell in two consecutive timeslots (in $\frac{kW}{h}$).
η_f^{FC}	Efficiency of the fth fuel cell.
Δt	Duration of the operating timeslots.
Δj	Duration of the intra-hour operating timeslots.
N^S	Number of scenarios.
$\Delta P_{s,t,j}^{ED}$	Error of forecasting electrical load in RT horizon.
$GS_g^{\mathrm{P2G,Min}}$	Minimum capacity of the gas storage system.
$GS_g^{\mathrm{P2G,Max}}$	Maximum capacity of the gas storage system.
$Q_b^{\mathrm{B,Min}}$	Minimum generation of the boiler.
$Q_b^{\mathrm{B,Max}}$	Maximum generation of the boiler.
$\rho_t^{\mathrm{G,N,DA}}$	Gas price.
$\rho_t^{\mathrm{WM,DA}}$	DA electricity market price.
$\bar{\rho}_{t,j}^{\mathrm{WM,RM}}$	Expected value of RM price.

$P_t^{\mathrm{WM,RM,Max}}$ Maximum trade with the RM.

$\eta_c^{\mathrm{CHP,H}}$ Thermal efficiency of the CHP.

$\eta_c^{\mathrm{CHP,E}}$ Electrical efficiency of the CHP.

R^H Gas constant (in $\frac{J}{mol\,K}$)

C_v^{HV} The capacity of the vth HV's hydrogen tank (m^3).

η_g^{P2G} Efficiency of the gth P2G storage.

(P_c^x, Q_c^x) Coordinates of the feasible operation region for the cth CHP unit $\forall x \in \{A,\ B,\ C,\ and\ D\}$ in (MW, $MWth$).

$P_g^{\mathrm{P2G,Max}}$ Maximum capacity of the P2G.

$G_g^{\mathrm{P2G,Dch,Max}}$ Maximum discharging gas from the gas storage system.

$H_v^{\mathrm{HV,Ini}}$ The amount of hydrogen in the vth HV's hydrogen tank at the arrival time.

η_b^{B} Efficiency of the boiler.

$H_t^{\mathrm{HV,DA}}$ Hydrogen required by hydrogen vehicles at the tth operating timeslot.

$\Delta_{\max}^{WM,RM}$ Maximum deviation from the expected WM prices.

H_v^{HV} Hydrogen required by the HV.

$H_{s,t,j}^{\mathrm{HV,RM}}$ Total amount of hydrogen required in RT.

D. Variables:

$\beta_{s,g,t,j}^{\mathrm{P2G,Up}}$ Binary variable indicating RU of the P2G.

$\beta_{s,g,t,j}^{\mathrm{P2G,D}}$ Binary variable indicating RD of the P2G.

$P_{s,g,t,j}^{\mathrm{P2G,Up}}$ RU of the P2G.

$P_{s,g,t,j}^{\mathrm{P2G,D}}$ RD of the P2G.

$GS_{g,t-1}^{\mathrm{P2G,DA}}$ State of charge of the gas storage system in DA.

$G_{s,g,t,j}^{\mathrm{P2G,Ch,Up}}$ RU of the gas charging the gas storage system.

$G_{s,g,t,j}^{\mathrm{P2G,Ch,D}}$ RD of the gas charging the gas storage system.

$GS_{s,g,t,j}^{\mathrm{P2G,RM}}$ State of charge of the gas storage system in RT.

$G_{s,g,t,j}^{\mathrm{P2G,Dch,Up}}$ RU of the gas discharging the gas storage system.

$G_{s,g,t,j}^{\mathrm{P2G,Dch,D}}$ RD of the gas discharging the gas storage system.

$Q_{b,t}^{\mathrm{B,DA}}$ Generated heat by the boiler in DA.

$Q_{s,b,t,j}^{\mathrm{B,UP}}$ RU of the boiler.

$Q_{s,b,t,j}^{\mathrm{B,D}}$ RD of the boiler.

$G_{s,b,t,j}^{\mathrm{B,UP}}$ RU of gas entering the boiler.

$G_{s,b,t,j}^{\mathrm{B,D}}$ RD of gas entering the boiler.

$G_{b,t}^{\mathrm{B,DA}}$ Gas entering the boiler in DA.

$\beta_{b,t}^{\mathrm{B,DA}}$ Binary variable indicating heat production of the boiler in DA.

$\beta_{s,b,t,j}^{\mathrm{B,Up}}$ Binary variable indicating RU of the boiler.

$\beta_{s,b,t,j}^{\mathrm{B,D}}$ Binary variable indicating RD of the boiler.

$H_{f,t}^{\mathrm{FC,In,DA}}$ Hydrogen feeding the FC in DA.

$P_{s,f,t,j}^{\mathrm{FC,Up}}$ RU of the FC generation.

$P_{s,f,t,j}^{\mathrm{FC,D}}$ RD of the FC generation.

$H_{s,f,t,j}^{\mathrm{FC,In,UP}}$ RU of hydrogen feeding the FC.

$H_{s,f,t,j}^{\mathrm{FC,In,D}}$ RD of hydrogen feeding the FC.

$\beta_{s,f,t,j}^{\mathrm{FC,Up}}$ Binary variable indicating RU of the FC.

$\beta_{s,f,t,j}^{\mathrm{FC,D}}$ Binary variable indicating RD of the FC.

$G_{s,t,j}^{\mathrm{N,Up}}$	RU of the gas entering the EH.
$G_{s,t,j}^{\mathrm{N,D}}$	RD of the gas entering the EH.
$G_{t}^{\mathrm{N,DA}}$	Gas entering the EH in DA.
$P_{s,e,t,j}^{\mathrm{Elz,Up}}$	RU of the electrolyzer.
$P_{s,e,t,j}^{\mathrm{Elz,D}}$	RD of the electrolyzer.
$H_{s,e,t,j}^{\mathrm{Elz,UP}}$	RU of the hydrogen released by the electrolyzer.
$H_{s,e,t,j}^{\mathrm{Elz,D}}$	RD of the hydrogen released by the electrolyzer.
$\beta_{s,c,t,j}^{\mathrm{Elz,Up}}$	Binary variable indicating RU of the electrolyzer.
$\beta_{s,c,t,j}^{\mathrm{Elz,D}}$	Binary variable indicating RD of the electrolyzer.
$H_{h,t}^{\mathrm{HT,DA,In}}$	Hydrogen entering the HT in DA.
$H_{h,t}^{\mathrm{HT,DA,Out}}$	Hydrogen coming out the HT in DA.
$H_{s,h,t,j}^{\mathrm{HT,RM,Out}}$	Hydrogen entering the HT in RT.
$H_{s,h,t,j}^{\mathrm{PHT,RM}}$	Hydrogen coming out the HT in RT.
$\beta_{s,t,j}^{\mathrm{WM,Up}}$	Binary variable indicating RU of purchase from the electricity market.
$\beta_{s,t,j}^{\mathrm{WM,D}}$	Binary variable indicating RD of purchase from the electricity market.
$P_{t}^{\mathrm{WM,DA,B}}$	Purchased electricity from the electricity market in DA.
$\rho_{t}^{\mathrm{WM,DA}}$	DA electricity market price.
$\rho_{t,j}^{\mathrm{WM,RM}}$	RM electricity price.
$P_{s,t,j}^{\mathrm{WM,Up}}$	RU of the interaction with RM.
$P_{s,t,j}^{\mathrm{WM,D}}$	RD of the interaction with RM.

$Q_{c,t}^{\mathrm{CHP,DA}}$ Thermal output of the CHP in DA time horizon.

$Q_{s,c,t,j}^{\mathrm{CHP,Up}}$ RU of thermal output of the CHP.

$Q_{s,c,t,j}^{\mathrm{CHP,D}}$ RD of thermal output of the CHP.

$P_{s,c,t,j}^{\mathrm{CHP,Up}}$ RU of the electrical output of the CHP.

$P_{s,c,t,j}^{\mathrm{CHP,D}}$ RD of the electrical output of the CHP.

$\beta_{s,c,t,j}^{\mathrm{CHP,Up}}$ Binary variable indicating RU of the CHP.

$\beta_{s,c,t,j}^{\mathrm{CHP,D}}$ Binary variable indicating RD of the CHP.

$\beta_{c,t}^{\mathrm{CHP,DA}}$ Binary variable indicating DA generation of the CHP.

$G_{s,c,t,j}^{\mathrm{CHP,UP}}$ RU of the gas entering the CHP.

$G_{s,c,t,j}^{\mathrm{CHP,D}}$ RD of the gas entering the CHP.

$P_{c,t}^{\mathrm{CHP,DA}}$ Electrical output of the CHP in DA time horizon.

$G_{c,t}^{\mathrm{CHP,DA}}$ Gas entering the CHP in DA time horizon.

$P_{e,t}^{\mathrm{Elz,DA}}$ Electricity consumed by the eth electrolyzer at the tth operating timeslot.

$H_{e,t}^{\mathrm{Elz,DA}}$ Hydrogen produced by the eth electrolyzer at the tth operating timeslot.

$H_{h,t}^{\mathrm{PHT,DA}}$ Hydrogen pressure of the hth hydrogen tank at the tth operating timeslot.

$P_{f,t}^{\mathrm{FC,DA}}$ Electricity generated by the fth fuel cell at the tth operating timeslot.

$P_{g,t}^{\mathrm{P2G,DA}}$ Power input of the gth P2G at the tth operating timeslot.

$G_{g,t}^{\mathrm{P2G,Ch,DA}}$ The amount of gas injected to the gth P2G storage at the tth operating timeslot.

$G_{g,t}^{\mathrm{P2G,Dch,DA}}$ The amount of gas used from the gth P2G storage at the tth operating timeslot.

$GS_{g,t}^{\mathrm{P2G,DA}}$ The amount of gas in the gth P2G storage at the tth operating timeslot.

E. Abbreviations:

EH	Energy hub.
HRS	Hydrogen refueling station.
HV	Hydrogen Vehicle.
RO	Robust optimization.
SP	Stochastic programming.
MILP	Mixed-integer linear programming.
DR	Demand response.
CHP	Combined heat and power.
P2G	Power-to-gas.
IGDT	Information gap decision theory.
PV	Photovoltaic.
FC	Fuel cell.
AT	Arrival time.
HT	Hydrogen tank.
Elz	Electrolyzer.
WM	Wholesale market.
ESS	Energy storage system.

DA	Day-ahead market.
RM	Regulation market.
RU	Regulation up.
RD	Regulation down.
RT	Real-time.

1. Introduction

The sustainable development of energy infrastructures aims at moving toward a clean and carbon-neutralized generation and operation concerning climate change over the decades. Hydrogen energy is taken into account as a green, clean and rich energy having a great potential to be developed in the future [1]. Due to the advantages of hydrogen vehicles over electric vehicles, such as high refueling speed, their penetration in cities is unavoidable. Therefore, hydrogen vehicles are being penetrated into cities as one of the most influential and promising ways for decarbonization of the transportation sector. As a result, the development of hydrogen fuel stations that can refill hydrogen vehicles is underway. Even though hydrogen technologies as well as P2X technologies are expensive at this time, they hold great potential for achieving a sustainable and low-carbon energy system and transportation system in the long run in order to move toward 100% clean energy. Besides, the concept of the energy hub (EH) is actually a noticeable solution to the demand for a continuous increase of energy consumption [2]. Recently, many types of units have been proposed to be integrated into EH, such as combined cooling, heat and power, chillers, fuel cells, boilers, electric vehicles or P2X technologies [3] and different storage systems like electricity, heat, gas, hydrogen, etc. [4]. Especially the interest in increasing the penetration of hydrogen-based technology in energy hubs can be indicated [5]. Thus, this article includes hydrogen as the main element of EH to minimize the total operation costs in the day-ahead (DA) and real-time (RT) horizons,

where the regulation market (RM) is run over the RT horizon. Dealing with the RM is crucial to compensate for the errors stemming from the DA decisions.

1.1. Literature Review

Recent literature also discusses the hydrogen-based technologies in energy systems and EHs. The integration of hydrogen storage in electricity, heating, and cooling system was investigated in [6] in order to boost the performance of the energy operation and increase the synergic efficiency of energy systems. Authors in [7] focused on the robust optimization of hydrogen-based integrated systems under carbon trading and including economical and environmentally advantageous. The optimal planning and operation of networked energy systems integrated with green hydrogen were proposed in [8] under intermittent wind power, solar irradiation as well as demand uncertainty. To meet the goal of carbon neutrality, a limitation was considered for CO2 production during the operation of resources, i.e., oil and natural gas.

The effect of the hydrogen storage system on the performance of an EH was investigated in [9] developing stochastic programming to take into account the uncertainties. This paper aimed to include the unit commitment problem in the operation of an EH concerning the start-up/shut-down constraints of unit commitment. In the paper [10], scenario-based stochastic programming (SP) was applied for handling the fluctuations of electricity price and RES in hydrogen-storage-based EH. The mixed-integer linear programming (MILP) was used to perform multi-objective scheduling EH to assure economic and environmental benefits. The paper [11] discussed the EH in the North Sea as a concept of offshore energy storage. The paper aimed to determine production quantities and efficiencies of electric energy from wind turbines, hydrogen, and ammonia. The paper [12] presented a two-stage coordinated volt-pressure optimization for integrated energy systems cooperated with EH. It considered a volt-VAR optimization functionality to reduce the impact of voltage deviation and ensure sufficient gas quality due to the hydrogen mixture. Additionally, the distributionally RO based on the Wasserstein metric was applied to consider

the renewable energy sources (RES) uncertainties. The paper [13] investigated the scheduling of an EH integrated with Power-to-Gas (P2G) storage, Power-to-Hydrogen, combined heat and power (CHP), wind power, boiler, and both heat and electrical storage considering demand response (DR). A scenario-based SP was used to consider the uncertainties of electricity prices and demands, as well as wind power. The aim of the model was to minimize the total operation cost of EH in the mean of a MILP problem. The paper [14] considered the EH to cover the electricity and heat demand of an islanded installation with the cooperation of battery and hydrogen storage systems, where RES and demand uncertainties were taken into account as a chance-constrained optimization problem and then reformulated as a RO problem. Thus, those bi-level operating strategy was realized as a day-ahead schedule optimization at the higher levels and then as model predictive control to track the schedules in real-time at lower levels. A hydrogen-based micro EH integrated with DR was proposed in [15] to minimize the total energy cost of EH in consideration of the uncertainty of electricity price by RO. Hydrogen storage and a fuel cell were included to satisfy the industrial hydrogen demands with the DA horizon.

The operation and planning of power systems have also been investigated by researchers to incorporate the application of hydrogen-based technologies to power systems. The article [16] presented the planning of a hydrogen refueling station that aimed to cover the demands of hydrogen vehicles (HVs) with the consideration of carbon emission flow, where nine-node hydrogen systems were addressed as a case study. Article [17] proposed an energy management system (EMS) based on hydrogen production that uses two kinds of DR, including conventional and P2X DR from electrolysis plants, hydrogen tank, electric battery, and hydrogen-consuming plants to maximize the profit of the EMS. The on-site local hydrogen production for hydrogen refueling station using RES was proposed in [18]. An optimal operation of an integrated power and hydrogen system was proposed in [19]. The main issue in the paper is to deliver hydrogen across the transportation network to satisfy time-varying demands. The hydrogen generation, delivery, and storage were optimized considering the capacity of

hydrogen tanks and routing costs.

Recently, in literature, the application of hybrid methods based on stochastic programming (SP), information gap decision theory (IGDT), or robust optimization (RO) to EH problems can be found. The combination of RO and SP can be found in [20]. Under the investigation, the SP was applied to develop the driving pattern uncertainties of EVs and RO to address the electricity market price uncertainties. Also, in [21] RO was applied to the same problem, but this time SP was applied to wind power. Then, in [22], the wind power uncertainties were included this time by RO, and the demands uncertainties of electric energy, heat, and gas were covered by SP. Additionally, in [23] SP was applied to the demand uncertainties issues, but wind power was covered by IGDT. Besides, the application of RO and IGDT can be found in [24]. RO was applied to model the uncertainty of electricity market prices and IGDT considers the wind power uncertainty. Another hybrid method is discussed in [25]. It shows the application of RO and SP to consider uncertainties of wind power, electricity market price, as well as electricity, heat, and natural gas demands.

1.2. Motivations and contributions

The literature review reveals valuable works related to the optimal operation of EHs. In addition, the literature discloses a new trend to include hydrogen technology in power systems. Although, based on the authors' knowledge, no study has considered hydrogen refueling stations and their uncertainties in the optimal operation of EHs so far. In addition, we have proposed the application of the hybrid-stochastic robust method to take into account the uncertainty of the real-time horizon dealing with the forecasting errors in intra-hours for the first time. It should be mentioned that the simultaneous operation of the DA and RM has previously been presented in [26] using pure stochastic programming disregarding the effect of new P2X technologies. However, we have developed the RO to consider the RM prices to reach the worst-case realization of the RM prices. In addition, it is proposed that uncertainties of HVs owners' behavior, which substantially affect the amount of hydrogen required at each operating timeslot

and intra-hour timeslot to refuel HVs, be managed by SP in an intra-hour timeslot. This seems essential because of the fact that the time required to refuel HVs is on the scale of several minutes; consequently, their uncertainties can not be effectively managed in DA with one-hour resolution planning. In other words, even if the amount of hydrogen required per hour is not uncertain, which it is, since the distribution of the HVs referred to refueling stations may not be uniform over an hour, the amount of hydrogen produced by the electrolyzer as well as the pressure of the hydrogen tank have to be rescheduled in a time resolution of approximately equal to the time required to refuel HVs. Besides, due to the fluctuations in both sides of generation and consumption, it is necessary to reschedule the decisions over minute horizons. By doing so, first, the EH operator can make decisions for the DA time horizon with the one-hour resolution, and then, the uncertainties of HVs, errors of demands, and RM prices are managed in a 10-minute resolution. Such a hybrid RO-SP model not only assures consideration of the worst-case realization of the electricity prices but also reduces the computational burden of the optimization problem. This is because, the SP is developed to take into account a part of the uncertainties, while the other part (RM prices) is addressed through the RO. Therefore, the number of variables that are a function of scenarios reduces. In order to have a comprehensive overview of the existing gap and the literature, the comparison of the proposed method and the literature in terms of the deployed P2X, type of the market, and the deployed mathematical approach is given in Table 1. To sum up, the contributions of the paper are summarized as follows:

- The uncertainties of hydrogen refueling stations have been developed through stochastic programming in an operation problem for the first time.
- The application of the hybrid stochastic-robust method has been proposed in a real-time horizon to cope with the uncertainties of the RM prices and HVs behavior as well as demands in intra-hours by an MILP formulation.
- Developing RM to take into account the HVs refueling in a real-time horizon, which has not been studied so far. It is necessary to develop the

Table 1: Overview of the literature review and the deployed hydrogen elements

Reference	Year	Hydrogen and P2X elements	DA market	RM	Mathematical approach
[6]	2022	Electrolyzer, FC	✗	✗	particle swarm optimization
[7]	2022	Electrolyzer, HT	✓	✗	RO
[8]	2022	Electrolyzer	✓	✗	deterministic
[9]	2022	Electrolyzer, HT, HRS	✓	✗	SP
[10]	2021	Electrolyzer, HT, FC	✓	✗	SP
[11]	2021	Electrolyzer, HT	✓	✗	deterministic
[12]	2021	P2G	✓	✗	distributionally RO
[13]	2020	P2G	✓	✗	SP
[14]	2020	Electrolyzer, HT, FC	✗	✗	chance constraint method
[15]	2020	Electrolyzer, HT, FC	✓	✗	RO
[16]	2021	Electrolyzer, HRS	✓	✗	genetic algorithm
[17]	2021	Electrolyzer, HT	✓	✗	deterministic
[18]	2020	Electrolyzer, HRS	✓	✗	SP
[19]	2021	Electrolyzer, HT	✓	✗	SP
[20]	2021	✗	✓	✗	hybrid RO + SP
[21]	2020	Electrolyzer, HT	✓	✗	SP
[22]	2021	Electrolyzer, HT	✓	✗	hybrid RO + SP
[23]	2021	Electrolyzer	✓	✗	hybrid IGDT + SP
[24]	2021	✗	✓	✗	hybrid IGDT + RO
[25]	2021	Electrolyzer, HT	✓	✗	hybrid RO + SP
[26]	2020	✗	✓	✓	SP
Proposed method	—	Electrolyzer, HT, FC, P2G	✓	✓	hybrid RO + SP

charging of HVs in short-time horizons due to the fast charging nature of HVs.

1.3. Paper organization

The rest of this paper is organized as follows. The problem description is given in Section II. The system model describing the mathematical models for hydrogen-based energy hubs' components, including electrolyzer, hydrogen tank, fuel cell, hydrogen vehicles, power-to-gas, CHP, and battery energy storage systems is given in Section III. In addition, the uncertainty characterization model is presented in Section III. The proposed model is developed in Section IV. The solution methodology is presented in Section V. Section VI is dedicated

to case studies and numerical results. Finally, the conclusion is given in Section VII.

2. Problem description

The EH is a trending concept that considers different kinds of energy carriers. Recently, the penetration of hydrogen-based technology has increased in power systems. Therefore, this paper addresses the optimal operation of EH considering the high penetration of hydrogen technology. In this work, a short-term operation of EH is taken into account in the regulation market. To be more exact, the decision is made after the realization of the DA electricity market and before RM. That is, the made decision might be subject to forecasting errors in intra-hours. The errors are compensated for in RM by RU/RD actions. In the EH understudy, as shown in Fig. 1, there are hydrogen-based devices, including an electrolyzer, which generates H_2 (hydrogen) from electricity, a hydrogen tank that stores hydrogen, a P2G storage system that stores natural gas after converting the electricity to natural gas, and a Fuel Cell (FC) which is fed by hydrogen and generates electricity. Besides, a CHP unit that is fed by gas generates electricity and heat at the same time and a boiler only generates heat. There are three types of output in the mentioned EH. The electricity demands are met through the CHP, the electricity market directly, and the FC. The heat demands are satisfied by the CHP and the boiler. In addition, there is a hydrogen station that consumes hydrogen to refuel the hydrogen vehicles (HV). The EH receives electricity from the electricity market and gas from the natural gas network. The EH is operated by the hub manager, who is the owner of the hub's assets and tries to minimize the total energy procurement cost of the energy carriers for the consumers. Under the mentioned conditions, the EH operator faces the uncertainty of the electricity market prices in RM, the driving pattern of the hydrogen vehicles, as well as electricity and heat demands. The driving pattern affects the initial state of charge of the HVs and the arrival time (AT) of the vehicles. The RO is deployed to reach the worst-case realization of the electricity

prices in RM. On the other hand, the stochastic nature of the driving pattern and stochastic forecasting errors of the demands are developed through the stochastic programming (SP) approach. The resulting framework is a hybrid robust-stochastic method to minimize the total operation cost of procuring the energy carriers in both DA and RT horizons while satisfying the output demands of the EH on a short-term horizon.

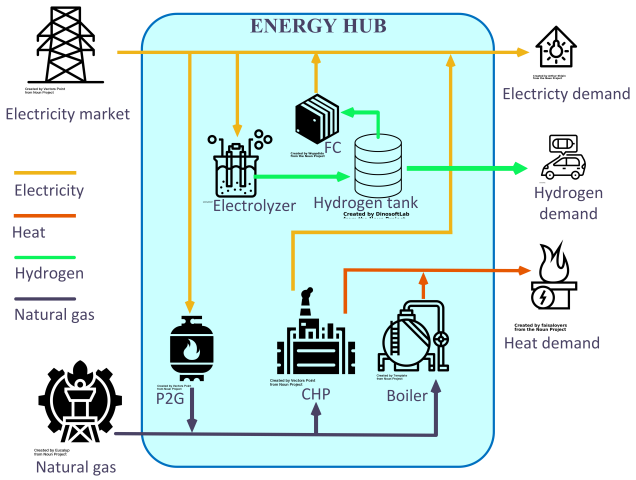

Figure 1: Hydrogen-based EH under study

3. System model

In this section, a mathematical model of the energy hub's components, including electrolyzers, hydrogen tanks, fuel cells, hydrogen vehicles, power-to-gas storage system, and CHP is presented. The interconnection of these components has been shown in Fig. 1.

3.1. Electrolyzer

Electrolyzers produce hydrogen by electrolyzing water using electricity [27]. Produced hydrogen (in kg) by electrolyzers can be formulated as (1) [28, 29].

$$H_{e,t}^{\mathrm{Elz,DA}} = \frac{\eta_e^{\mathrm{Elz}} P_{e,t}^{\mathrm{Elz,DA}}}{L^{\mathrm{HV,H}}}, \quad \forall t \in \mathcal{T}, \quad \forall e \in \mathcal{E}. \tag{1}$$

The electrical power consumed by the electrolyzers has to be in its permissible range. In addition, the ability to decrease and increase the power consumption of the electrolyzer in two consecutive operating timeslots is limited [27].These limitations have been formulated in equations (2), and (3), respectively.

$$P_e^{\mathrm{Elz,Min}} \leq P_{e,t}^{\mathrm{Elz,DA}} \leq P_e^{\mathrm{Elz,Max}}, \quad \forall t \in \mathcal{T}, \quad \forall e \in \mathcal{E}. \tag{2}$$

$$\kappa_e^{\mathrm{Elz,Min}} \Delta t \leq P_{e,t}^{\mathrm{Elz,DA}} - P_{e,t-1}^{\mathrm{Elz,DA}} \leq \kappa_e^{\mathrm{Elz,Max}} \Delta t, \quad \forall t \in \mathcal{T}, \quad \forall e \in \mathcal{E}. \tag{3}$$

Constraints that are imposed to electrolyzers by RM can be formulated as (4) to (12). Eqs. (4) and ((5)) restrict the RU and RD actions, respectively. Eqs. (6) and ((8)) guarantee that RU and RD do not happen simultaneously. The released hydrogen for RU and RD are given in (9) and (10), respectively. Ramp rate constraints for RU and RD of the electrolyzer are indicated in (11) and (12), respectively.

$$P_{e,t}^{\mathrm{Elz,DA}} + P_{s,e,t,j}^{\mathrm{Elz,Up}} \leq P_e^{\mathrm{Elz,Max}}, \quad \forall t \in \mathcal{T},\ e \in \mathcal{E},\ s \in \S, j \in \mathcal{T}_t, \tag{4}$$

$$P_{e,t}^{\mathrm{Elz,DA}} - P_{s,e,t,j}^{\mathrm{Elz,D}} \geq P_e^{\mathrm{Elz,Min}}, \quad \forall t \in \mathcal{T},\ e \in \mathcal{E},\ s \in \S, j \in \mathcal{T}_t, \tag{5}$$

$$P_{s,e,t,j}^{\mathrm{Elz,Up}} \leq P_e^{\mathrm{Elz,Max}} \beta_{s,c,t,j}^{\mathrm{Elz,Up}}, \quad \forall t \in \mathcal{T},\ e \in \mathcal{E},\ s \in \S, j \in \mathcal{T}_t, \tag{6}$$

$$P_{s,e,t,j}^{\mathrm{Elz,D}} \leq P_e^{\mathrm{Elz,Max}} \beta_{s,c,t,j}^{\mathrm{Elz,D}}, \quad \forall t \in \mathcal{T},\ e \in \mathcal{E},\ s \in \S, j \in \mathcal{T}_t, \tag{7}$$

$$\beta_{s,c,t,j}^{\mathrm{Elz,D}} + \beta_{s,c,t,j}^{\mathrm{Elz,Up}} \leq 1, \quad \forall t \in \mathcal{T},\ e \in \mathcal{E},\ s \in \S, j \in \mathcal{T}_t, \tag{8}$$

$$H_{s,e,t,j}^{\mathrm{Elz,UP}} = (\frac{\eta_e^{\mathrm{Elz}}}{L^{\mathrm{HV,H}}}) P_{s,e,t,j}^{\mathrm{Elz,Up}}, \quad \forall t \in \mathcal{T},\ e \in \mathcal{E},\ s \in \S, j \in \mathcal{T}_t, \tag{9}$$

$$H_{s,e,t,j}^{\mathrm{Elz,D}} = (\frac{\eta_e^{\mathrm{Elz}}}{L^{\mathrm{HV,H}}}) P_{s,e,t,j}^{\mathrm{Elz,D}}, \quad \forall t \in \mathcal{T},\ e \in \mathcal{E},\ s \in \S, j \in \mathcal{T}_t, \tag{10}$$

$$\kappa_e^{\mathrm{Elz,Min}} \Delta j \leq P_{s,e,t,j}^{\mathrm{Elz,Up}} - P_{s,e,t,j-1}^{\mathrm{Elz,Up}} \leq \kappa_e^{\mathrm{Elz,Max}} \Delta j\ , \quad \forall t \in \mathcal{T},\ e \in \mathcal{E},\ s \in \S, j \in \mathcal{T}_t, \tag{11}$$

$$\kappa_e^{\mathrm{Elz,Min}} \Delta j \leq P_{s,e,t,j}^{\mathrm{Elz,D}} - P_{s,e,t,j-1}^{\mathrm{Elz,D}} \leq \kappa_e^{\mathrm{Elz,Max}} \Delta j\ , \quad \forall t \in \mathcal{T},\ e \in \mathcal{E},\ s \in \S, j \in \mathcal{T}_t, \tag{12}$$

3.2. Hydrogen tank

The hydrogen produced by the electrolyzer is stored in a high-pressure hydrogen tank after compression by the compressor. The hydrogen stored in this tank provides the ability for the energy hub owner to produce and store hydrogen at times when energy is cheaper and sell it to hydrogen vehicles while the electricity prices are high [27]. At steady state, the hydrogen inflow rate of the hydrogen tank equals to hydrogen molar production rate of the electrolyzer [30].

$$H_{h,t}^{\mathrm{HT,DA,In}} = \sum_{e \in \mathcal{E}} \chi_{e,h} H_{e,t}^{\mathrm{Elz,DA}}, \quad \forall t \in \mathcal{T}, \quad \forall h \in \mathcal{H}. \tag{13}$$

$$H_{h,t}^{\mathrm{PHT,DA}} = H_{h,t-1}^{\mathrm{PHT,DA}} + \frac{R^H T_{h,t}^{\mathrm{HT}}}{V_h^{\mathrm{HT}} Mol^{\mathrm{H}}} (H_{h,t}^{\mathrm{HT,DA,In}} - H_{h,t}^{\mathrm{HT,DA,Out}}), \quad \forall t \in \mathcal{T}, \quad \forall h \in \mathcal{H}. \tag{14}$$

The hydrogen tanks' pressures have to be in the permissible ranges

$$H_h^{\mathrm{PHT,Min}} \leq H_{h,t}^{\mathrm{PHT,DA}} \leq H_h^{\mathrm{PHT,Max}}, \quad \forall t \in \mathcal{T}, \quad \forall h \in \mathcal{H}. \tag{15}$$

where $\mathcal{H}$ is the set of hydrogen tanks. $H_h^{\mathrm{PHT,Min}}$ and $H_h^{\mathrm{PHT,Max}}$ are the minimum, and maximum permissible pressure of the kth hydrogen tank, respectively. $H_{h,t}^{\mathrm{PHT,DA}}$ is the pressure of the kth hydrogen tank at the tth operating timeslot. It should be noted that the hydrogen pressure calculated by (14) is in $\frac{N}{m^2}$, which equals to Pa; and, 1 bar equals to $10^5 Pa$.

Eq. (14) indicates the pressure at each hour is equal to the previous hour's pressure plus the pressure obtained by the DA action. The HT pressure is bounded by (15).

Hydrogen tanks' constraints that have to be taken into account in RM are formulated by (16) to (18). The hydrogen pressure balance is indicated in (16). Since there are two types of scheduling, including DA and RT scheduling, the HT pressure can only change within the interval scheduled DA storage. It imposes the uniqueness of the HT during scheduling. The hydrogen pressure in the HT should respect the minimum and maximum capacity in (18).

$$H_{s,h,t,j}^{\mathrm{PHT,RM}} = H_{s,h,t,j-1}^{\mathrm{PHT,RM}} + (\frac{R^H T_{h,t}^{\mathrm{HT}}}{V_h^{\mathrm{HT}} Mol^{\mathrm{H}}}) \cdot (H_{s,e,t,j}^{\mathrm{Elz,UP}} - H_{s,e,t,j}^{\mathrm{Elz,D}}) - H_{s,h,t,j}^{\mathrm{HT,RM,Out}}, \quad \forall t \in \mathcal{T},\ h \in \mathcal{H},\ s \in \S, j \in \mathcal{T}_t, \tag{16}$$

$$H_{s,h,t-1,j_6}^{\mathrm{PHT,RM}} = H_{h,t}^{\mathrm{PHT,DA}}, \quad \forall t \in \mathcal{T},\ h \in \mathcal{H},\ s \in \S, \tag{17}$$

$$H_h^{\mathrm{PHT,Min}} \leq H_{s,h,t,j}^{\mathrm{PHT,RM}} \leq H_h^{\mathrm{PHT,Max}} \quad \forall t \in \mathcal{T},\ h \in \mathcal{H},\ s \in \S,\ j \in \mathcal{T}_t \tag{18}$$

3.3. Fuel cell

The energy hub's owner can use the hydrogen stored in the high-pressure tank to generate electricity by fuel cells. The electric power generated by fuel cells can be modeled by (19). The power output of the fuel cells is limited by (20); moreover, the ability to decrease and increase the electrical power generated by fuel cells in two consecutive operating timeslots is limited [31]. This limitation has been formulated by (21).

$$P_{f,t}^{\mathrm{FC,DA}} = L^{\mathrm{HV,H}} \eta_f^{\mathrm{FC}} H_{f,t}^{\mathrm{FC,In,DA}}, \quad \forall t \in \mathcal{T}, \quad \forall f \in \mathcal{F}. \tag{19}$$

$$P_f^{\mathrm{FC,Min}} \leq P_{f,t}^{\mathrm{FC,DA}} \leq P_f^{\mathrm{FC,Max}}, \quad \forall t \in \mathcal{T}, \quad \forall f \in \mathcal{F}. \tag{20}$$

$$\kappa_f^{\mathrm{FC,Min}} \Delta t \leq P_{f,t}^{\mathrm{FC,DA}} - P_{f,t-1}^{\mathrm{FC,DA}} \leq \kappa_f^{\mathrm{FC,Max}} \Delta t, \quad \forall t \in \mathcal{T}, \quad \forall f \in \mathcal{F}. \tag{21}$$

Constraints imposed by RM to FCs are modeled by (22) to (30).

$$P_{s,f,t,j}^{\mathrm{FC,Up}} = L^{\mathrm{HV,H}} \eta_f^{\mathrm{FC}} H_{s,f,t,j}^{\mathrm{FC,In,UP}} \quad \forall t \in \mathcal{T},\ f \in \mathcal{F},\ s \in \S,\ j \in \mathcal{T}_t \tag{22}$$

$$P_{s,f,t,j}^{\mathrm{FC,D}} = L^{\mathrm{HV,H}} \eta_f^{\mathrm{FC}} H_{s,f,t,j}^{\mathrm{FC,In,D}} \quad \forall t \in \mathcal{T},\ f \in \mathcal{F},\ s \in \S,\ j \in \mathcal{T}_t \tag{23}$$

$$P_{f,t}^{\mathrm{FC,DA}} + P_{s,f,t,j}^{\mathrm{FC,Up}} \leq P_f^{\mathrm{FC,Max}} \quad \forall t \in \mathcal{T},\ f \in \mathcal{F},\ s \in \S,\ j \in \mathcal{T}_t \tag{24}$$

$$P_{f,t}^{\mathrm{FC,DA}} - P_{s,f,t,j}^{\mathrm{FC,D}} \geq P_f^{\mathrm{FC,Min}} \quad \forall t \in \mathcal{T},\ f \in \mathcal{F},\ s \in \S,\ j \in \mathcal{T}_t \tag{25}$$

$$P_{s,f,t,j}^{\mathrm{FC,Up}} \leq P_f^{\mathrm{FC,Max}} \beta_{s,f,t,j}^{\mathrm{FC,Up}} \quad \forall t \in \mathcal{T},\ f \in \mathcal{F},\ s \in \S,\ j \in \mathcal{T}_t \tag{26}$$

$$P_{s,f,t,j}^{\mathrm{FC,D}} \leq P_f^{\mathrm{FC,Max}} \beta_{s,f,t,j}^{\mathrm{FC,D}} \quad \forall t \in \mathcal{T},\ f \in \mathcal{F},\ s \in \S,\ j \in \mathcal{T}_t \tag{27}$$

$$\beta_{s,f,t,j}^{\mathrm{FC,D}} + \beta_{s,f,t,j}^{\mathrm{FC,Up}} \leq 1 \quad \forall t \in \mathcal{T},\ f \in \mathcal{F},\ s \in \S,\ j \in \mathcal{T}_t \tag{28}$$

$$\kappa_f^{\mathrm{FC,Min}} \Delta j \leq P_{s,f,t,j}^{\mathrm{FC,Up}} - P_{s,f,t,j-1}^{\mathrm{FC,Up}} \leq \kappa_f^{\mathrm{FC,Max}} \Delta j, \quad \forall t \in \mathcal{T},\ f \in \mathcal{F},\ s \in \S,\ j \in \mathcal{T}_t \tag{29}$$

$$\kappa_f^{\mathrm{FC,Min}}\Delta j \le P_{s,f,t,j}^{\mathrm{FC,D}} - P_{s,f,t,j-1}^{\mathrm{FC,D}} \le \kappa_f^{\mathrm{FC,Max}}\Delta j, \quad \forall t \in \mathcal{T},\ f \in \mathcal{F},\ s \in \S,\ j \in \mathcal{T}_t \tag{30}$$

3.4. Hydrogen vehicles

The amount of hydrogen required per hour of the day-ahead to refuel hydrogen vehicles depends on the number of hydrogen vehicles referred to the HRS and the amount of hydrogen required by each of them. Equation (31) models the total hydrogen required at hour t of the day-ahead. In this equation, $\mathcal{V}_t \subset \mathcal{V}$; and, to satisfy the preferences of HVs' owners, the hydrogen level of HVs when leaving the HRSs have to be at its maximum level. Accordingly, the amount of hydrogen required by the HRS at hour t of the day-ahead is a function of the number of HVs referred to the HRS at that hour and the initial amount of hydrogen in their HV's hydrogen tank when they arrived at the HRS. This has been modeled by equation (32). The actual realization of the hydrogen demand in real-time, which has been taken into account in RM, is modeled by (33).

$$H_t^{\mathrm{HV,DA}} = \sum_{v \in \mathcal{V}_t} H_v^{\mathrm{HV}}, \quad \forall t \in \mathcal{T} \tag{31}$$

$$H_v^{\mathrm{HV}} = C_v^{\mathrm{HV}} - H_v^{\mathrm{HV,Ini}}, \quad \forall v \in \mathcal{V} \tag{32}$$

$$H_{s,t,j}^{\mathrm{HV,RM}} = \sum_{v \in \mathcal{V}_t^{RM}} H_v^{\mathrm{HV}}, \quad \forall t \in \mathcal{T}, s \in \S, j \in \mathcal{T}_t. \tag{33}$$

3.5. P2G model

The P2G storage technology is an upcoming new technology that concerns gas production from electricity. The main process of converting electricity to natural gas has two main steps. First, to electrolyze water by electricity and generating hydrogen (H_2), and next, combining the produced hydrogen by CO_2 to generate CH_4. The second step is known as methanation in chemical actions. Afterward, the produced methane is compressed and injected into the natural

gas network [32]. Since the input electricity always is under severe fluctuation of the electricity market, it is worth storing the gas during off-peak hours and injecting it into the natural gas network during peak hours of natural gas. The following equations declare the gas generated through the electricity in (34) and storing it in the gas storage system in (35). Obviously, the amount of gas in each hour depends on the amount of gas in the previous hour, charging and discharging gas from the P2G storage system.

$$G_{g,t}^{\mathrm{P2G,Ch,DA}} = \eta_g^{\mathrm{P2G}} P_{g,t}^{\mathrm{P2G,DA}}, \quad \forall t \in \mathcal{T}, \quad \forall g \in \mathcal{G}, \tag{34}$$

$$\begin{aligned} GS_{g,t}^{\mathrm{P2G,DA}} = GS_{g,t-1}^{\mathrm{P2G,DA}} + G_{g,t}^{\mathrm{P2G,Ch,DA}} \\ - G_{g,t}^{\mathrm{P2G,Dch,DA}}, \quad \forall t \in \mathcal{T}, \quad \forall g \in \mathcal{G}. \end{aligned} \tag{35}$$

Constraints that are imposed by RM to P2Gs are formulated by equations (36) to (48).

$$\begin{aligned} G_{s,g,t,j}^{\mathrm{P2G,Ch,Up}} - G_{s,g,t,j}^{\mathrm{P2G,Ch,D}} = \eta_g^{\mathrm{P2G}} (P_{s,g,t,j}^{\mathrm{P2G,Up}} \\ - P_{s,g,t,j}^{\mathrm{P2G,D}}), \quad \forall t \in \mathcal{T},\ g \in \mathcal{G},\ s \in \S,\ j \in \mathcal{T}_t, \end{aligned} \tag{36}$$

$$\begin{aligned} GS_{s,g,t,j}^{\mathrm{P2G,RM}} = GS_{s,g,t,j-1}^{\mathrm{P2G,RM}} + (G_{s,g,t,j}^{\mathrm{P2G,Ch,Up}} - \\ G_{s,g,t,j}^{\mathrm{P2G,Ch,D}}) + (G_{s,g,t,j}^{\mathrm{P2G,Dch,Up}} - G_{s,g,t,j}^{\mathrm{P2G,Dch,D}}), \\ \forall t \in \mathcal{T},\ g \in \mathcal{G},\ s \in \S,\ j \in \mathcal{T}_t, \end{aligned} \tag{37}$$

$$\begin{aligned} P_{g,t}^{\mathrm{P2G,DA}} + P_{s,g,t,j}^{\mathrm{P2G,Up}} \le P_g^{\mathrm{P2G,Max}}, \\ \forall t \in \mathcal{T},\ g \in \mathcal{G},\ s \in \S,\ j \in \mathcal{T}_t, \end{aligned} \tag{38}$$

$$\begin{aligned} G_{g,t}^{\mathrm{P2G,Dch,DA}} + G_{s,g,t,j}^{\mathrm{P2G,Dch,Up}} \le G_g^{\mathrm{P2G,Dch,Max}}, \\ \forall t \in \mathcal{T},\ g \in \mathcal{G},\ s \in \S,\ j \in \mathcal{T}_t, \end{aligned} \tag{39}$$

$$\begin{aligned} P_{g,t}^{\mathrm{P2G,DA}} + P_{s,g,t,j}^{\mathrm{P2G,D}} \le 0, \\ \forall t \in \mathcal{T},\ g \in \mathcal{G},\ s \in \S,\ j \in \mathcal{T}_t, \end{aligned} \tag{40}$$

$$\begin{aligned} G_{g,t}^{\mathrm{P2G,Dch,DA}} - G_{s,g,t,j}^{\mathrm{P2G,Dch,D}} \ge 0, \\ \forall t \in \mathcal{T},\ g \in \mathcal{G},\ s \in \S,\ j \in \mathcal{T}_t, \end{aligned} \tag{41}$$

$$GS_{g}^{\mathrm{P2G,Min}} \leq GS_{g,t}^{\mathrm{P2G,DA}} \leq GS_{g}^{\mathrm{P2G,Max}}, \quad \forall t \in \mathcal{T},\ g \in \mathcal{G},\ s \in \S,\ j \in \mathcal{T}_t, \tag{42}$$

$$GS_{g}^{\mathrm{P2G,Min}} \leq GS_{s,g,t,j}^{\mathrm{P2G,RM}} \leq GS_{g}^{\mathrm{P2G,Max}}, \quad \forall t \in \mathcal{T},\ g \in \mathcal{G},\ s \in \S,\ j \in \mathcal{T}_t, \tag{43}$$

$$G_{s,g,t,j}^{\mathrm{P2G,Dch,Up}} \leq G_{g}^{\mathrm{P2G,Dch,Max}} \beta_{s,g,t,j}^{\mathrm{P2G,Up}}, \quad \forall t \in \mathcal{T},\ g \in \mathcal{G},\ s \in \S,\ j \in \mathcal{T}_t, \tag{44}$$

$$G_{s,g,t,j}^{\mathrm{P2G,Dch,D}} \leq G_{g}^{\mathrm{P2G,Dch,Max}} \beta_{s,g,t,j}^{\mathrm{P2G,D}}, \quad \forall t \in \mathcal{T},\ g \in \mathcal{G},\ s \in \S,\ j \in \mathcal{T}_t, \tag{45}$$

$$GS_{s,g,t,j_0}^{\mathrm{P2G,RM}} = GS_{s,g,t-1,j_6}^{\mathrm{P2G,RM}}, \quad \forall t \in \mathcal{T},\ g \in \mathcal{G},\ s \in \S, \tag{46}$$

$$GS_{s,g,t_0,j}^{\mathrm{P2G,RM}} = GS_{s,g,t_{24},j}^{\mathrm{P2G,RM}}, \quad \forall t \in \mathcal{T},\ g \in \mathcal{G},\ s \in \S,\ j \in \mathcal{T}_t, \tag{47}$$

$$GS_{g,t}^{\mathrm{P2G,DA}} = GS_{s,g,t,j_0}^{\mathrm{P2G,RM}}, \quad \forall t \in \mathcal{T},\ g \in \mathcal{G},\ s \in \S, \tag{48}$$

3.6. Boiler Model

The boiler is fed by natural gas, and its heat is obtained through its conversion coefficient. For instance, the heat generated in the DA horizon is given as follows:

$$Q_{b,t}^{\mathrm{B,DA}} = \eta_{b}^{\mathrm{B}} G_{b,t}^{\mathrm{B,DA}}, \quad \forall t \in \mathcal{T},\ b \in \mathcal{B}. \tag{49}$$

The heat generated by the boiler is restricted by its bounds in (50). Eqs. (51)-(51) declare that either RU or RD occurs at the same time. The amount of RU and RD of the boiler is limited by its generated value in DA. The boiler can reduce its generation up to the maximum value of the DA in (54), and it can increase the generation by RU as much as it respects the capacity of the boiler based on (55).

$$Q_b^{\mathrm{B,Min}} \cdot \beta_{b,t}^{\mathrm{B,DA}} \leq Q_{b,t}^{\mathrm{B,DA}} \leq Q_b^{\mathrm{B,Max}} \cdot \beta_{b,t}^{\mathrm{B,DA}}, \quad \forall t \in \mathcal{T},\ b \in \mathcal{B}, \tag{50}$$

$$Q_b^{\mathrm{B,Min}} \cdot \beta_{s,b,t,j}^{\mathrm{B,D}} \leq Q_{s,b,t,j}^{\mathrm{B,D}} \leq Q_b^{\mathrm{B,Max}} \cdot \beta_{s,b,t,j}^{\mathrm{B,D}}, \quad \forall t \in \mathcal{T},\ b \in \mathcal{B},\ s \in \S,\ j \in \mathcal{T}_t, \tag{51}$$

$$Q_b^{\mathrm{B,Min}} \cdot \beta_{s,b,t,j}^{\mathrm{B,Up}} \leq Q_{s,b,t,j}^{\mathrm{B,UP}} \leq Q_b^{\mathrm{B,Max}} \cdot \beta_{s,b,t,j}^{\mathrm{B,Up}}, \quad \forall t \in \mathcal{T},\ b \in \mathcal{B},\ s \in \S,\ j \in \mathcal{T}_t, \tag{52}$$

$$\beta_{s,b,t,j}^{\mathrm{B,D}} + \beta_{s,b,t,j}^{\mathrm{B,Up}} \leq 1 \quad \forall t \in \mathcal{T},\ b \in \mathcal{B},\ s \in \S,\ j \in \mathcal{T}_t, \tag{53}$$

$$Q_{s,b,t,j}^{\mathrm{B,D}} \leq Q_{b,t}^{\mathrm{B,DA}} \quad \forall t \in \mathcal{T},\ b \in \mathcal{B},\ s \in \S,\ j \in \mathcal{T}_t, \tag{54}$$

$$Q_b^{\mathrm{B,Max}} \cdot \beta_{b,t}^{\mathrm{B,DA}} - Q_{b,t}^{\mathrm{B,DA}} - Q_{s,b,t,j}^{\mathrm{B,UP}} \geq 0 \quad \forall t \in \mathcal{T},\ b \in \mathcal{B},\ s \in \S,\ j \in \mathcal{T}_t, \tag{55}$$

3.7. CHP model

The amount of electricity and heat generated by CHP depends on the amount of gas entering the CHP. This is the same rule for DA outputs and RD and RU actions as given in (56) -(61)

$$P_{c,t}^{\mathrm{CHP,DA}} = G_{c,t}^{\mathrm{CHP,DA}} \eta_c^{\mathrm{CHP,E}}, \quad \forall t \in \mathcal{T},\ c \in \mathcal{C}, \tag{56}$$

$$Q_{c,t}^{\mathrm{CHP,DA}} = G_{c,t}^{\mathrm{CHP,DA}} \eta_c^{\mathrm{CHP,H}}, \quad \forall t \in \mathcal{T},\ c \in \mathcal{C}, \tag{57}$$

$$P_{s,c,t,j}^{\mathrm{CHP,D}} = G_{c,t}^{\mathrm{CHP,DA}} \eta_c^{\mathrm{CHP,E}}, \quad \forall t \in \mathcal{T},\ c \in \mathcal{C}\ s \in \S,\ j \in \mathcal{T}_t, \tag{58}$$

$$Q_{s,c,t,j}^{\mathrm{CHP,D}} = G_{s,c,t,j}^{\mathrm{CHP,D}} \eta_c^{\mathrm{CHP,H}}, \quad \forall t \in \mathcal{T},\ c \in \mathcal{C}\ s \in \S,\ j \in \mathcal{T}_t, \tag{59}$$

$$P^{\mathrm{CHP,Up}}_{s,c,t,j} = G^{\mathrm{CHP,UP}}_{s,c,t,j}\eta^{\mathrm{CHP,E}}_{c}, \quad \forall t \in \mathcal{T},\ c \in \mathcal{C}\ s \in \S,\ j \in \mathcal{T}_t, \tag{60}$$

$$Q^{\mathrm{CHP,Up}}_{s,c,t,j} = G^{\mathrm{CHP,UP}}_{s,c,t,j}\eta^{\mathrm{CHP,H}}_{c}, \quad \forall t \in \mathcal{T},\ c \in \mathcal{C}\ s \in \S,\ j \in \mathcal{T}_t, \tag{61}$$

The electrical and thermal outputs of CHP units are mutually dependent. This dependency is generally defined by a feasible operation (FOR) region. To define the FOR, a closed area is determined through sets of coordination showing the amount of output of the electricity and heat as given in Fig. 2. For instance, $(P^{\mathrm{A}}_c, Q^{\mathrm{A}}_c)$ in the figure means the amount of electricity in coordinates A. By considering the coordinates $A(0, 247)$, $B(180, 215)$, $C(104.8, 81)$ and $D(0, 98.8)$, the constraints (62)-(74) show the FOR for both DA and RM constraints.

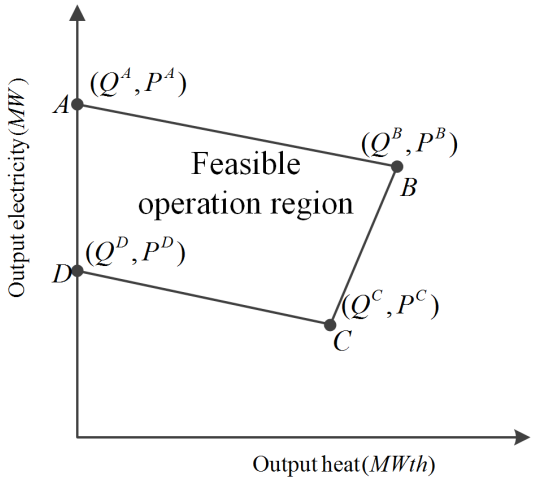

Figure 2: Feasible operation region for the CHP unit [33]

$$P^{\mathrm{CHP,DA}}_{c,t} \cdot \eta^{\mathrm{CHP,E}}_{c} + 0.177 P^{\mathrm{CHP,DA}}_{c,t} \cdot \eta^{\mathrm{CHP,H}}_{c} \leq 247\beta^{\mathrm{CHP,DA}}_{c,t}, \quad \forall t \in \mathcal{T},\ c \in \mathcal{C}, \tag{62}$$

$$P^{\mathrm{CHP,DA}}_{c,t} \cdot \eta^{\mathrm{CHP,E}}_{c} - 1.782 P^{\mathrm{CHP,DA}}_{c,t} \cdot \eta^{\mathrm{CHP,H}}_{c} \geq -105.71\beta^{\mathrm{CHP,DA}}_{c,t}, \quad \forall t \in \mathcal{T},\ c \in \mathcal{C}, \tag{63}$$

$$P_{c,t}^{\mathrm{CHP,DA}} \cdot \eta_c^{\mathrm{CHP,E}} + 0.1698 P_{c,t}^{\mathrm{CHP,DA}} \cdot \eta_c^{\mathrm{CHP,H}} \geq 98.8 \beta_{c,t}^{\mathrm{CHP,DA}}, \quad \forall t \in \mathcal{T},\ c \in \mathcal{C}, \tag{64}$$

$$P_{s,c,t,j}^{\mathrm{CHP,Up}} \cdot \eta_c^{\mathrm{CHP,E}} + 0.177 P_{s,c,t,j}^{\mathrm{CHP,Up}} \cdot \eta_c^{\mathrm{CHP,H}} \leq 247 \beta_{s,c,t,j}^{\mathrm{CHP,Up}}, \quad \forall t \in \mathcal{T},\ c \in \mathcal{C}\ s \in \S,\ j \in \mathcal{T}_t, \tag{65}$$

$$P_{s,c,t,j}^{\mathrm{CHP,Up}} \cdot \eta_c^{\mathrm{CHP,E}} - 1.782 P_{s,c,t,j}^{\mathrm{CHP,Up}} \cdot \eta_c^{\mathrm{CHP,H}} \geq -105.71 \beta_{s,c,t,j}^{\mathrm{CHP,Up}}, \quad \forall t \in \mathcal{T},\ c \in \mathcal{C}\ s \in \S,\ j \in \mathcal{T}_t, \tag{66}$$

$$P_{s,c,t,j}^{\mathrm{CHP,Up}} \cdot \eta_c^{\mathrm{CHP,E}} + 0.1698 P_{s,c,t,j}^{\mathrm{CHP,Up}} \cdot \eta_c^{\mathrm{CHP,H}} \geq 98.8 \beta_{s,c,t,j}^{\mathrm{CHP,Up}}, \quad \forall t \in \mathcal{T},\ c \in \mathcal{C}\ s \in \S,\ j \in \mathcal{T}_t, \tag{67}$$

$$P_{s,c,t,j}^{\mathrm{CHP,D}} \cdot \eta_c^{\mathrm{CHP,E}} + 0.177 P_{s,c,t,j}^{\mathrm{CHP,D}} \cdot \eta_c^{\mathrm{CHP,H}} \leq 247 \beta_{s,c,t,j}^{\mathrm{CHP,D}}, \quad \forall t \in \mathcal{T},\ c \in \mathcal{C}\ s \in \S,\ j \in \mathcal{T}_t, \tag{68}$$

$$P_{s,c,t,j}^{\mathrm{CHP,D}} \cdot \eta_c^{\mathrm{CHP,E}} - 1.782 P_{s,c,t,j}^{\mathrm{CHP,D}} \cdot \eta_c^{\mathrm{CHP,H}} \geq -105.71 \beta_{s,c,t,j}^{\mathrm{CHP,D}}, \quad \forall t \in \mathcal{T},\ c \in \mathcal{C}\ s \in \S,\ j \in \mathcal{T}_t, \tag{69}$$

$$P_{s,c,t,j}^{\mathrm{CHP,D}} \cdot \eta_c^{\mathrm{CHP,E}} + 0.1698 P_{s,c,t,j}^{\mathrm{CHP,D}} \cdot \eta_c^{\mathrm{CHP,H}} \geq 98.8 \beta_{s,c,t,j}^{\mathrm{CHP,D}}, \quad \forall t \in \mathcal{T},\ c \in \mathcal{C}\ s \in \S,\ j \in \mathcal{T}_t, \tag{70}$$

$$\beta_{s,c,t,j}^{\mathrm{CHP,D}} + \beta_{s,c,t,j}^{\mathrm{CHP,Up}} \leq 1, \quad \forall t \in \mathcal{T},\ c \in \mathcal{C}\ s \in \S,\ j \in \mathcal{T}_t, \tag{71}$$

$$(P_{c,t}^{\mathrm{CHP,DA}} - P_{s,c,t,j}^{\mathrm{CHP,D}} + P_{s,c,t,j}^{\mathrm{CHP,Up}}) \cdot \eta_c^{\mathrm{CHP,E}} + 0.177 (P_{c,t}^{\mathrm{CHP,DA}} - P_{s,c,t,j}^{\mathrm{CHP,D}} + P_{s,c,t,j}^{\mathrm{CHP,Up}}) \cdot \eta_c^{\mathrm{CHP,H}} \leq 247 \beta_{s,c,t,j}^{\mathrm{CHP,D}}, \quad \forall t \in \mathcal{T},\ c \in \mathcal{C}\ s \in \S,\ j \in \mathcal{T}_t, \tag{72}$$

$$(P_{c,t}^{\mathrm{CHP,DA}} - P_{s,c,t,j}^{\mathrm{CHP,D}} + P_{s,c,t,j}^{\mathrm{CHP,Up}}) \cdot \eta_c^{\mathrm{CHP,E}} - 1.782 (P_{c,t}^{\mathrm{CHP,DA}} - P_{s,c,t,j}^{\mathrm{CHP,D}} + P_{s,c,t,j}^{\mathrm{CHP,Up}}) \cdot \eta_c^{\mathrm{CHP,H}} \geq -105.71 \beta_{s,c,t,j}^{\mathrm{CHP,D}}, \quad \forall t \in \mathcal{T},\ c \in \mathcal{C}\ s \in \S,\ j \in \mathcal{T}_t, \tag{73}$$

$$
\begin{aligned}
&(P_{c,t}^{\mathrm{CHP,DA}} - P_{s,c,t,j}^{\mathrm{CHP,D}} + P_{s,c,t,j}^{\mathrm{CHP,Up}}) \cdot \eta_c^{\mathrm{CHP,E}} + \\
&0.1698(P_{c,t}^{\mathrm{CHP,DA}} - P_{s,c,t,j}^{\mathrm{CHP,D}} + P_{s,c,t,j}^{\mathrm{CHP,Up}}) \cdot \eta_c^{\mathrm{CHP,H}} \\
&\geq 98.8\beta_{s,c,t,j}^{\mathrm{CHP,D}}, \quad \forall t \in \mathcal{T},\ c \in \mathcal{C}\ s \in \S,\ j \in \mathcal{T}_t,
\end{aligned} \tag{74}
$$

3.8. Uncertainty modelling

The robust optimization model is deployed to reach the worst-case realization of the electricity price uncertainty. To do so, the positive and negative deviation of the electricity prices should be maximized to reach the worst case as shown in (75). It should be noted that all electricity purchased should be included: RU/RD to compensate for the electricity demands, RU/RD for the input electricity of the P2G units as well as RU/RD of the electrolyzer. The negative/positive deviation has to be taken into account for addressing both options of purchasing and selling to the electricity market. The amount of deviation plus the expected value denotes the worst case of the electricity prices in (76). The amount of deviation in each hour is limited in (77). The total amount of uncertainty during the time horizon is bounded by the uncertainty budget in (78) and (79).

$$
\begin{aligned}
&\max_{\phi_{\rho t}} \sum_{t\in\mathcal{T}} \sum_{j\in\mathcal{T}_t} \rho_{t,j}^{\mathrm{WM,RM}} \big[(P_{s,t,j}^{\mathrm{WM,Up}} - P_{s,t,j}^{\mathrm{WM,D}}) + \\
&\sum_{g\in\mathcal{G}} (P_{s,g,t,j}^{\mathrm{P2G,Up}} - P_{s,g,t,j}^{\mathrm{P2G,D}}) + \sum_{e\in\mathcal{E}} (P_{s,e,t,j}^{\mathrm{Elz,Up}} - P_{s,e,t,j}^{\mathrm{Elz,D}})\big], \\
&\qquad\qquad \forall t \in \mathcal{T},
\end{aligned} \tag{75}
$$

$$
\rho_{t,j}^{\mathrm{WM,RM}} = \bar{\rho}_{t,j}^{\mathrm{WM,RM}} + \phi_{\rho t} \quad : \xi_t \,\epsilon\, \mathcal{R}, \quad \forall t \in \mathcal{T} \tag{76}
$$

$$
\begin{aligned}
&\mid \phi_{\rho t} \mid \leq \Delta_{\max}^{WM,RM} \bar{\rho}_{t,j}^{\mathrm{WM,RM}} \quad : \underline{\varphi}_t \leq 0,\ \overline{\varphi}_t \geq 0, \\
&\qquad\qquad\qquad\qquad\qquad\qquad \forall t \in \mathcal{T},
\end{aligned} \tag{77}
$$

$$
\sum_{t\in\mathcal{T}} \mid \phi_{\rho t} \mid \leq \Gamma^p \quad : \underline{\varpi} \geq 0,\ \sigma_t \,\epsilon\, \mathcal{R}, \quad \forall t \in \mathcal{T} \tag{78}
$$

$$\Gamma^{p} = N_p \Delta_{\max}^{WM,RM} \frac{\sum_{t\in\mathcal{T}} \sum_{j\in\mathcal{T}_t} \bar{\rho}_{t,j}^{\mathrm{WM,RM}}}{N_T} \tag{79}$$

Due to the existence of non-linearity comes from the absolute value function in Eq. (77) and (78), the method presented in [24] is deployed to linearize the relations. Next, the duality theory is applied to get the equivalent min-objective function as given in Eqs. (80)-(84), where (80) denotes the objective function and (81)-(84) represent the new dual constraints.

$$\begin{aligned} \min \sum_{t\in\mathcal{T}} \sum_{j\in\mathcal{T}_t} \bar{\rho}_{t,j}^{\mathrm{WM,RM}} \xi_t + \Delta_{\max}^{WM,RM} \bar{\rho}_{t,j}^{\mathrm{WM,RM}} \bar{\varphi}_t - \\ \Delta_{\max}^{WM,RM} \bar{\rho}_{t,j}^{\mathrm{WM,RM}} \underline{\varphi}_t + \Gamma\varpi, \quad \forall t \in \mathcal{T},\ j \in \mathcal{T}_t, \end{aligned} \tag{80}$$

$$\begin{aligned} \xi_{t,j} \geq \frac{1}{N^S} \sum_{s\in\S} \pi_s \sum_{m\in\mathcal{M}} \Big((P_{s,t,j}^{\mathrm{WM,Up}} - P_{s,t,j}^{\mathrm{WM,D}}) \\ + \sum_{g\in\mathcal{G}} (P_{s,g,t,j}^{\mathrm{P2G,Up}} - P_{s,g,t,j}^{\mathrm{P2G,D}}) + \sum_{e\in\mathcal{E}} (P_{s,e,t,j}^{\mathrm{Elz,Up}} - \\ P_{s,e,t,j}^{\mathrm{Elz,D}}) \Big), \quad \forall t \in \mathcal{T},\ s \in \S,\ j \in \mathcal{T}_t, \end{aligned} \tag{81}$$

$$-\xi_{t,j} + \bar{\varphi}_{t,j} + \underline{\varphi}_{t,j} + \sigma_{t,j} = 0, \quad \forall t \in \mathcal{T},\ j \in \mathcal{T}_t, \tag{82}$$

$$-\sigma_{t,j} + \varpi \geq 0, \quad \forall t \in \mathcal{T},\ j \in \mathcal{T}_t, \tag{83}$$

$$\sigma_{t,j} + \varpi \geq 0, \quad \forall t \in \mathcal{T},\ j \in \mathcal{T}_t, \tag{84}$$

In the proposed model, the severe uncertainties of the hydrogen vehicles' deriving patterns as well as the forecasting errors of demands have been managed by a stochastic approach. A normal distribution function with a mean value of zero has been used to generate the errors of heat and electricity demands. The stochastic programming approach has been deployed to address the mentioned uncertainties. Hence, the uncertainties are represented by the scenario concept. To do so, each scenario contains the data on the initial state of charge of HVs ($H_v^{\mathrm{HV,Ini}}$), the arrival time of HVs (AT), and electricity demand deviation

($\Delta P^{ED}_{s,t,j}$), and heat demand deviation ($\Delta P^{HD}_{s,t,j}$). Each scenario vector SV is represented as follows:

$$SV = [H_v^{\mathrm{HV,Ini}} \quad AT \quad \Delta P^{ED}_{s,t,j} \quad \Delta P^{HD}_{s,t,j}] \tag{85}$$

That is, the final scenarios are obtained by the combination of the mentioned uncertainty sources. Obviously, due to the large number of scenarios after the combination of multiple sources, an appropriate scenario reduction method is required in order to meet the tractability of commercial solvers.

4. Proposed model

As mentioned in Section 2, the uncertainty of the electricity market prices is considered through the RO, while the uncertainty of the driving pattern of HVs and the errors of the demands are taken into account by SP. The RO optimization part recasts in the objective function as follows:

The uncertainty of the HVs is included after this step. Totally, the following steps are proposed for the proposed framework.

- Step 1: presenting (75)-(79) as the objective function to reach the worst case realization of the electricity price uncertainty.
- Step 2: linearizing the absolute value function in the price uncertainty model, see [24].
- Step 3: using duality theory to obtain the min-objective presented in (80)-(84)
- Step 4: adding (80)-(84) to the RM objective presented in (88).

The objective function includes both the DA and RM costs as given in (86). The DA cost is obtained by considering the cost of electricity procurement from the DA market and the cost of purchasing natural gas from the natural gas network as mentioned in (87). The RM cost is calculated based on the RU and RD actions with the intra-hours, where RU is treated as a cost and RD is like a benefit, as given in (88). It should be noted that the robust cost of dealing with

the RM is added here due to the developing uncertainty of the RM prices by the RO approach.

$$
\begin{aligned}
&\min_{D_{\mathrm{DA}}, D_{\mathrm{RM}}} \quad \sum_{t \in \mathcal{T}} \Big(\mathrm{Cost}_t^{\mathrm{DA}} + E\big(\sum_{j \in \mathcal{T}_t} \mathrm{Cost}_{t,j}^{\mathrm{RM}}\big) \Big) \\
&\quad \text{subjected to} \\
&\qquad \text{electrolyzers constraints :} \quad (2) - (3), \\
&\qquad \text{hydrogen tanks constraints :} \quad (14) - (15), \\
&\qquad \text{fuel cells constraints :} \quad (20) - (21), \\
&\qquad \text{hydrogen vehicle constraints :} \quad (31) - (32), \\
&\qquad \text{CHP constraints :} \quad (56) - (74), \\
&\qquad \text{dual constraints :} \quad (81) - (84), \\
&\qquad \text{balance constraints :} \quad (96) - (102),
\end{aligned}
\tag{86}
$$

where

$$
\begin{aligned}
D_{\mathrm{DA}} &= \{Q_{b,t}^{\mathrm{B,DA}}, G_{b,t}^{\mathrm{B,DA}}, \beta_{b,t}^{\mathrm{B,DA}}, \\
&H_{f,t}^{\mathrm{FC,In,DA}}, G_t^{\mathrm{N,DA}}, H_{h,t}^{\mathrm{HT,DA,In}}, H_{h,t}^{\mathrm{HT,DA,Out}}, \\
&P_t^{\mathrm{WM,DA,B}}, \beta_{c,t}^{\mathrm{CHP,DA}}, Q_{c,t}^{\mathrm{CHP,DA}}, P_{c,t}^{\mathrm{CHP,DA}}, \\
&G_{c,t}^{\mathrm{CHP,DA}}, P_{e,t}^{\mathrm{Elz,DA}}, H_{e,t}^{\mathrm{Elz,DA}}, H_{h,t}^{\mathrm{PHT,DA}}, P_{f,t}^{\mathrm{FC,DA}} \\
&P_{g,t}^{\mathrm{P2G,DA}}, G_{g,t}^{\mathrm{P2G,Ch,DA}}, G_{g,t}^{\mathrm{P2G,Dch,DA}}, GS_{g,t}^{\mathrm{P2G,DA}}, \\
&: \forall t \in \mathcal{T}, c \in \mathcal{C}, h \in \mathcal{H}, b \in \mathcal{B}, f \in \mathcal{F}, e \in \mathcal{E}, g \in \mathcal{G}\}
\end{aligned}
$$

$$
\begin{aligned}
D_{\mathrm{RM}} &= \{\beta_{s,g,t,j}^{\mathrm{P2G,Up}}, \beta_{s,g,t,j}^{\mathrm{P2G,D}}, P_{s,g,t,j}^{\mathrm{P2G,Up}}, P_{s,g,t,j}^{\mathrm{P2G,D}}, \\
&G_{s,g,t,j}^{\mathrm{P2G,Ch,Up}}, G_{s,g,t,j}^{\mathrm{P2G,Ch,D}}, G_{s,g,t,j}^{\mathrm{P2G,Dch,D}}, G_{s,g,t,j}^{\mathrm{P2G,Dch,Up}}, \\
&Q_{s,b,t,j}^{\mathrm{B,UP}}, Q_{s,b,t,j}^{\mathrm{B,D}}, G_{s,b,t,j}^{\mathrm{B,UP}}, G_{s,b,t,j}^{\mathrm{B,D}}, \beta_{s,c,t,j}^{\mathrm{CHP,D}}, \beta_{s,b,t,j}^{\mathrm{B,Up}}, \\
&\beta_{s,b,t,j}^{\mathrm{B,D}}, P_{s,f,t,j}^{\mathrm{FC,Up}}, P_{s,f,t,j}^{\mathrm{FC,D}}, H_{s,f,t,j}^{\mathrm{FC,In,UP}}, H_{s,f,t,j}^{\mathrm{FC,In,D}}, \beta_{s,f,t,j}^{\mathrm{FC,Up}}, \\
&\beta_{s,f,t,j}^{\mathrm{FC,D}}, G_{s,t,j}^{\mathrm{N,Up}}, G_{s,t,j}^{\mathrm{N,D}}, P_{s,e,t,j}^{\mathrm{Elz,Up}}, P_{s,e,t,j}^{\mathrm{Elz,D}}, H_{s,e,t,j}^{\mathrm{Elz,UP}}, \\
&H_{s,e,t,j}^{\mathrm{Elz,D}}, \beta_{s,c,t,j}^{\mathrm{Elz,Up}}, \beta_{s,c,t,j}^{\mathrm{Elz,D}}, \beta_{s,t,j}^{\mathrm{WM,Up}}, \beta_{s,t,j}^{\mathrm{WM,D}}, P_{s,t,j}^{\mathrm{WM,Up}}, \\
&P_{s,t,j}^{\mathrm{WM,D}}, Q_{s,c,t,j}^{\mathrm{CHP,Up}}, Q_{s,c,t,j}^{\mathrm{CHP,D}}, P_{s,c,t,j}^{\mathrm{CHP,Up}}, P_{s,c,t,j}^{\mathrm{CHP,D}}, \\
&\beta_{s,c,t,j}^{\mathrm{CHP,Up}}, G_{s,c,t,j}^{\mathrm{CHP,UP}}, G_{s,c,t,j}^{\mathrm{CHP,D}}, \quad : \forall t \in \mathcal{T}, \\
&c \in \mathcal{C}, h \in \mathcal{H}, b \in \mathcal{B}, f \in \mathcal{F}, e \in \mathcal{E}, g \in \mathcal{G}, j \in \mathcal{T}_t\}
\end{aligned}
$$

$$
\begin{aligned}
\mathrm{Cost}_t^{\mathrm{DA}} = \rho_t^{\mathrm{WM,DA}} P_t^{\mathrm{WM,DA,B}} + \rho_t^{\mathrm{G,N,DA}} G_t^{\mathrm{N,DA}}, \\
\forall t \in \mathcal{T}
\end{aligned} \tag{87}
$$

$$
\begin{aligned}
\mathrm{Cost}_{t,j}^{\mathrm{RM}} = \bar{\rho}_{t,j}^{\mathrm{WM,RM}} \xi_{t,j} + \Delta_{\max}^{WM,RM} \bar{\rho}_{t,j}^{\mathrm{WM,RM}} \bar{\varphi}_{t,j} - \\
\Delta_{\max}^{WM,RM} \bar{\rho}_{t,j}^{\mathrm{WM,RM}} \underline{\varphi}_{t,j} + \Gamma + \rho_t^{\mathrm{G,N,RM}} \\
(G_{t,j}^{\mathrm{N,UP}} - G_{t,j}^{\mathrm{N,D}}), \quad \forall t \in \mathcal{T}, j \in \mathcal{T}_t
\end{aligned} \tag{88}
$$

Eqs. (91) and (92) indicate the gas balance for the RU and RD actions. Eqs. (89) and (90) show the gas balance for the DA and RT horizons. In RT horizons, the RU and RD actions compensate for the errors.

$$G_t^{\mathrm{N,DA}} + \sum_{g\in\mathcal{G}} G_{g,t}^{\mathrm{P2G,Dch,DA}} - \sum_{c\in\mathcal{C}} G_{c,t}^{\mathrm{CHP,DA}} - \sum_{b\in\mathcal{B}} G_{b,t}^{\mathrm{B,DA}} = 0, \quad \forall t \in \mathcal{T} \tag{89}$$

$$\begin{aligned} &G_{s,t,j}^{\mathrm{N,Up}} - G_{s,t,j}^{\mathrm{N,D}} + \sum_{g\in\mathcal{G}} (\\ &- G_{s,g,t,j}^{\mathrm{P2G,Dch,D}}) - \sum_{c\in\mathcal{C}} (G_{s,c,t,j}^{\mathrm{CHP,UP}} - G_{s,c,t,j}^{\mathrm{CHP,D}}) - \\ &\sum_{b\in\mathcal{B}} (G_{s,b,t,j}^{\mathrm{B,Up}} - G_{s,b,t,j}^{\mathrm{B,D}}) = 0, \quad \forall t \in \mathcal{T},\ s \in \S,\ j \in \mathcal{T}_t, \end{aligned} \tag{90}$$

$$G_{s,t,j}^{\mathrm{N,UP}} = \sum_{c\in\mathcal{C}} G_{s,c,t,j}^{\mathrm{CHP,UP}} + \sum_{b\in\mathcal{B}} G_{s,b,t,j}^{\mathrm{B,UP}}, \quad \forall t \in \mathcal{T},\ s \in \S,\ j \in \mathcal{T}_t, \tag{91}$$

$$G_{s,t,j}^{\mathrm{N,D}} = \sum_{c\in\mathcal{C}} G_{s,c,t,j}^{\mathrm{CHP,D}} + \sum_{b\in\mathcal{B}} G_{s,b,t,j}^{\mathrm{B,D}}, \quad \forall t \in \mathcal{T},\ s \in \S,\ j \in \mathcal{T}_t, \tag{92}$$

The DA and RM balance of the heat are given in (93) and (94), respectively.

$$\sum_{c\in\mathcal{C}} Q_{c,t}^{\mathrm{CHP,DA}} + \sum_{b\in\mathcal{B}} Q_{b,t}^{\mathrm{B,DA}} - \sum_{l\in\mathcal{L}} Q_{l,t}^{\mathrm{Demand}} = 0, \quad \forall t \in \mathcal{T}, \tag{93}$$

$$\begin{aligned} &\sum_{c\in\mathcal{C}} \eta_c^{\mathrm{CHP,H}} (G_{s,c,t,j}^{\mathrm{CHP,UP}} - G_{s,c,t,j}^{\mathrm{CHP,D}}) \\ &+ \sum_{b\in\mathcal{B}} \eta_b^{\mathrm{B}} (G_{s,b,t,j}^{\mathrm{B,UP}} - G_{s,b,t,j}^{\mathrm{B,D}}) = \Delta Q_{s,t,j}^{Demand}, \end{aligned} \tag{94}$$

$$\forall t \in \mathcal{T},\ s \in \S,\ j \in \mathcal{T}_t.$$

The DA balance of electricity is given in (95). The RM balance of electricity is represented in (96). As can be seen, the RM deviation is compensated by RU

and RD.

$$P_t^{\mathrm{WM,DA,B}} + \sum_{f\in\mathcal{F}} P_{f,t}^{\mathrm{FC,DA}} + \sum_{c\in\mathcal{C}} P_{c,t}^{\mathrm{CHP,DA}} - \sum_{g\in\mathcal{G}} P_{g,t}^{\mathrm{P2G,DA}} - \sum_{e\in\mathcal{E}} P_{e,t}^{\mathrm{Elz,DA}} = 0, \quad \forall t \in \mathcal{T} \tag{95}$$

$$P_{s,t,j}^{\mathrm{WM,Up}} - P_{s,t,j}^{\mathrm{WM,D}} + \sum_{f\in\mathcal{F}} (P_{s,f,t,j}^{\mathrm{FC,Up}} - P_{s,f,t,j}^{\mathrm{FC,D}}) + \sum_{c\in\mathcal{C}} (P_{s,c,t,j}^{\mathrm{CHP,Up}} - P_{s,c,t,j}^{\mathrm{CHP,D}}) = \Delta P_{s,t,j}^{ED}, \quad \forall t \in \mathcal{T},\ s \in \S,\ j \in \mathcal{T}_t, \tag{96}$$

The amount of RU and RD for the interaction with the electricity market are restricted by (97)-(100). Additionally, only one of the states of RU or RD can occur at the same time.

$$P_t^{\mathrm{WM,DA,B}} - P_{s,t,j}^{\mathrm{WM,D}} \geq 0, \quad \forall t \in \mathcal{T},\ s \in \S,\ j \in \mathcal{T}_t, \tag{97}$$

$$P_{s,t,j}^{\mathrm{WM,Up}} \leq P_t^{\mathrm{WM,RM,Max}} \beta_{s,t,j}^{\mathrm{WM,Up}}, \quad \forall t \in \mathcal{T},\ s \in \S,\ j \in \mathcal{T}_t, \tag{98}$$

$$P_{s,t,j}^{\mathrm{WM,D}} \leq P_t^{\mathrm{WM,RM,Max}} \beta_{s,t,j}^{\mathrm{WM,D}}, \quad \forall t \in \mathcal{T},\ s \in \S,\ j \in \mathcal{T}_t, \tag{99}$$

$$\beta_{s,t,j}^{\mathrm{WM,D}} + \beta_{s,t,j}^{\mathrm{WM,Up}} \leq 1, \quad \forall t \in \mathcal{T},\ s \in \S,\ j \in \mathcal{T}_t, \tag{100}$$

The hydrogen balance equation can be formulated as equation (102). The first term on the right side of this equation represents the total amount of hydrogen required to refuel hydrogen vehicles at the tth operating timeslot. The second and third terms on the right side of this equation model the total amount of consumed hydrogen by fuel cells, and the total industrial hydrogen loads at the tth operating timeslot, respectively.

$$\sum_{h\in\mathcal{H}} H_{h,t}^{\mathrm{HT,DA,Out}} = H_t^{\mathrm{HV,DA}} + \sum_{f\in\mathcal{F}} H_{f,t}^{\mathrm{FC,In,DA}}, \quad \forall t \in \mathcal{T}. \tag{101}$$

$$\sum_{h\in\mathcal{H}} H_{s,h,t,j}^{\mathrm{HT,RM,Out}} = H_{s,t,j}^{\mathrm{HV,RM}} + \sum_{f\in\mathcal{F}} (H_{s,f,t,j}^{\mathrm{FC,In,UP}} - H_{s,f,t,j}^{\mathrm{FC,In,D}}), \forall t \in \mathcal{T},\ s \in \S,\ j \in \mathcal{T}_t, \tag{102}$$

5. Case study and Discussions

5.1. Case study

The electrical and thermal loads over the DA and RT horizon are taken from [26] as shown in Figs. 3 and 4. For instance, the maximum deviation occurs in the time sample 41 for the electricity demands, which is 465 kWh deviation on the base of 3300 kW, which shows a 14% deviation. The positive and negative values in RT show the deviation from the DA values every 10 minutes. It should be mentioned that all the figures in RT horizon and RM are given by their expected values. Totally 100 HVs are considered for the hydrogen refueling station. For the sake of simplicity, their capacity is assumed similar, 4 kgs. Developing their behavior during 24-h, the required hydrogen for the DA horizon is depicted in Fig. 5-a. Since the forecasting of the number of HVs is always subject to uncertainty, the related error is shown in Fig. 5-b by positive/negative values for the required hydrogen in every 10 minutes. Besides, the initial state of charge of the HVs is subject to uncertainty in RT horizon, where its expected value is given in Fig. 5-c.

Table 2: Details of the devices in the understudy EH [34, 29]

Characteristic	Value	Characteristic	Value
$L^{\mathrm{HV,H}}$ (kWh/kg)	39.72	R^{H} (J/mol K)	8.314
$T_{h,t}^{\mathrm{HT}}$ (K)	313	V_{h}^{HT} (m^3)	200
$H_{h}^{\mathrm{PHT,Min}}$ (Pascal)	0	$H_{h}^{\mathrm{PHT,Max}}$(Pascal)	200000
η_{e}^{Elz}	0.6	Mol^{H}(kg/mol)	0.02
η_{f}^{FC}	0.7	$P_{e}^{\mathrm{Elz,Max}}$(kW)	2000
η_{g}^{P2G}	0.75	η_{b}^{B}	0.85

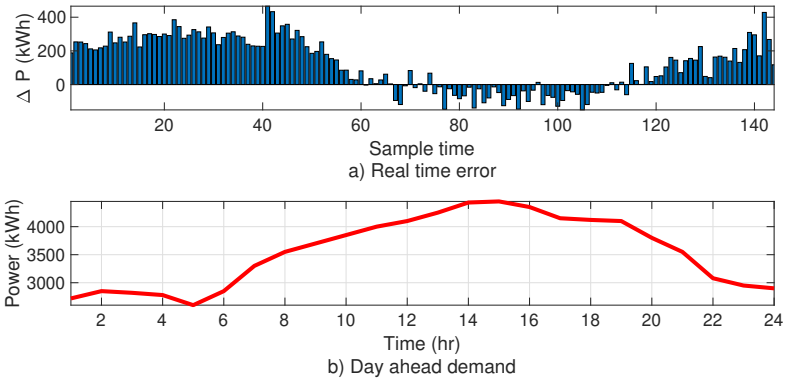

Figure 3: Electricity demands over real-time and day-ahead horizon

The electricity market prices for the RM are uncertain inputs where the RO approach is developed to address its uncertainty. The expected values of the RM prices are given in Fig. 6-a. The DA prices for the electricity market and natural gas are depicted in Fig. 6-b, where the gas prices are higher during hours 6-11 and 18. For the uncertainty sources, including electrical and thermal demand errors as well as the driving pattern of the HVs and the initial state of charge, five scenarios are considered for each. After the scenario combination, 625 scenarios resulted. The number of scenarios is limited to 10 by scenario reduction. The total number of HVs is 100. The feasible operation region of the CHP is considered 10 times bigger than the characteristics mentioned in [26]. The other characteristics of the problem, including the HT, P2G, CHP, and boiler details, are provided in Table 2.

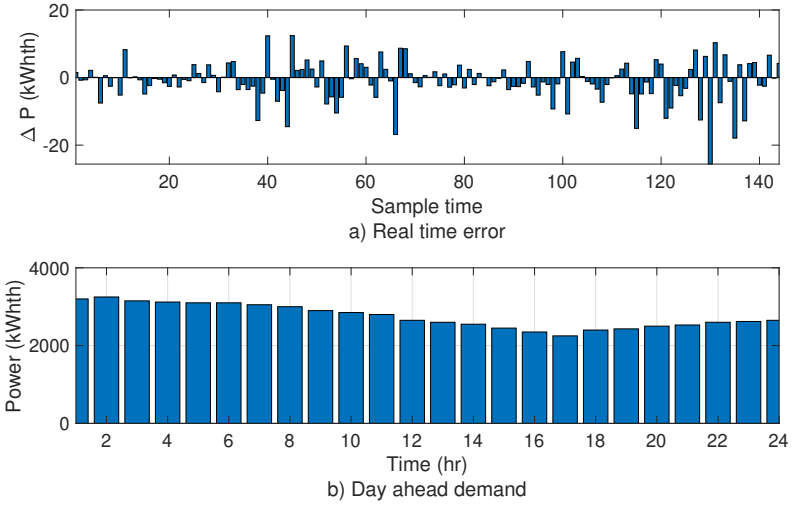

Figure 4: Heat demands over real-time and day-ahead horizon

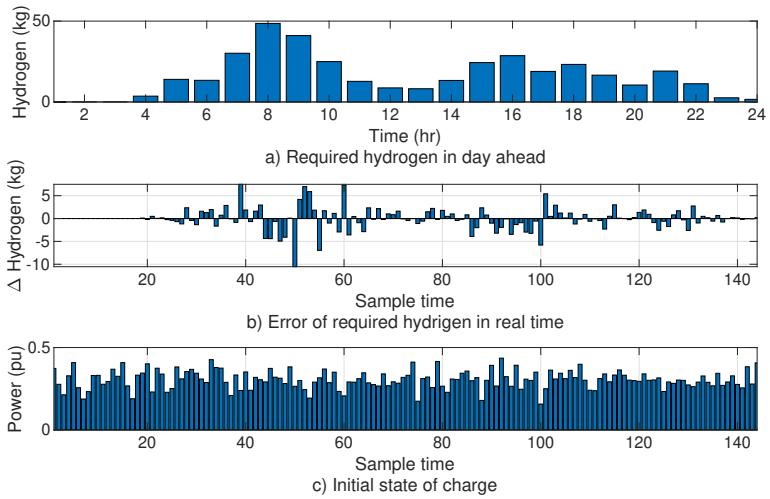

Figure 5: Required hydrogen for HVs over day-ahead and real-time horizon as well as initial state of charge of HVs

5.2. Discussions

The results are given in this subsection. It should be mentioned that the presented figures stand on the average values (expected) of the scenarios in all figures. In addition, the DA values are also shown by every 10 minutes to prepare a proper situation to compare the DA and RT horizons. Therefore, all figures dimension is 144 (24 hours multiplies by 6 intra-hours). It is worth mentioning that the RT values in the figures are obtained by adding the RU and subtracting the RD from DA values.

Given the input data, Fig. 7 demonstrates the amount of electricity purchased in DA and RM. As can be seen, the DA purchased does not change in intra-hours, while the operator increase/decrease the amount of purchase using regulation up/down actions to compensate for the errors given in Fig. 3. For instance, during intra-hours 67-114, the RD is activated to decrease the amount of purchased electricity in DA to compensate for the negative errors. A vice-versa action is seen for the other parts of the scheduling horizon by the positive errors. The purchased electricity from the electricity market is consumed by the demands, P2G, and the electrolyzer. As another example, the amount of purchase has been increased to 3580 kW in the RM, while it had been decided to purchase 3200 kW in the DA market, which is equal to a 10% increase. Fig. 8 shows the electricity consumed by the electrolyzer over the DA and RT horizons. There is a fluctuation in the beginning hours, where the RT decisions do not follow the DA decisions properly. To find out the reason, it is necessary to pay attention to the HV pattern in Fig. 5, where the first peak of required hydrogen is during 5-11 (31-72 intra-hours). That is, the HT should be ready to refuel the HVs. A decision is made in DA to inject hydrogen into the HT based on the DA electricity prices, but since there is a fluctuation in RM electricity prices in the mentioned beginning hours, and on average, the RM prices are lower during 1-60 in intra-hours, the operator increases its electricity purchase during the beginning hours (on average), to avoid increasing the purchase in peak hours of HV pattern dramatically.

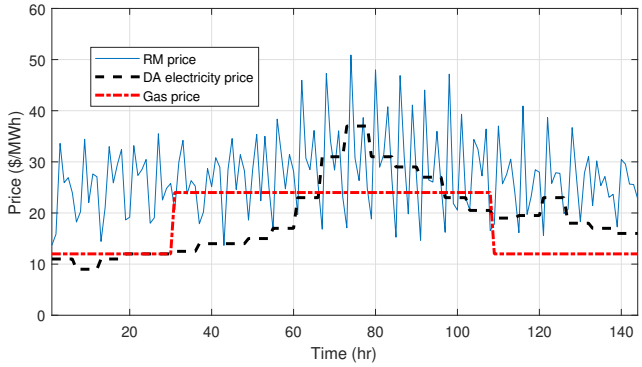

Figure 6: Gas and electricity prices

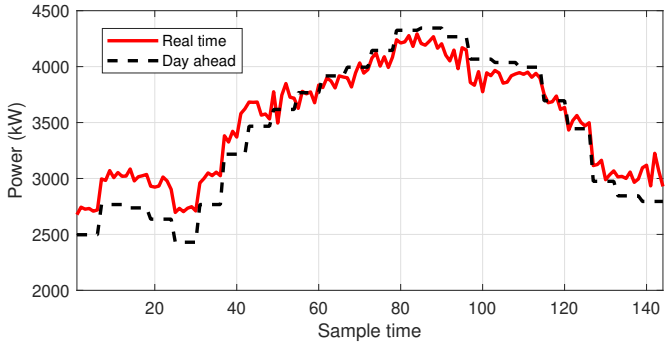

Figure 7: Traded electricity with the electricity market in the DA and RM

Fig. 9 depicts the hydrogen pressure in the HT and verifies the increase of the pressure during the beginning hours by activating RU for the electrolyzer. According to Fig. 10, the HT is discharged with a pattern similar to the HVs pattern if Fig. 5-a with two obvious peaks. It is worth mentioning that the RT discharge of the HT is always higher than or equal to the DA values, while there are some negative errors for the HVs required hydrogen. It is due to an increase in FC production during the RT horizon compared to the one of the DA as shown in Fig. 11. Indeed, the stored hydrogen is used to generate electricity by the FC to compensate for the electricity demands in RT.

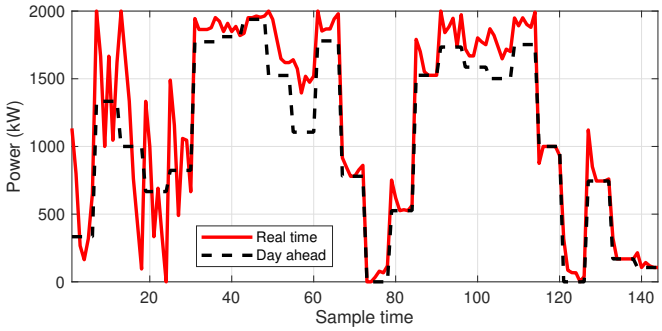

Figure 8: Consumed electricity by the electrolyzer

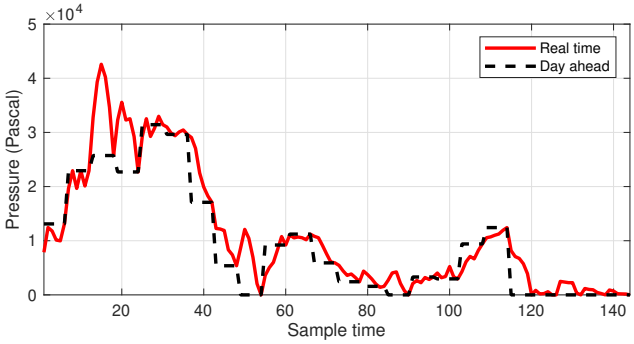

Figure 9: Level of hydrogen pressure in the hydrogen tank

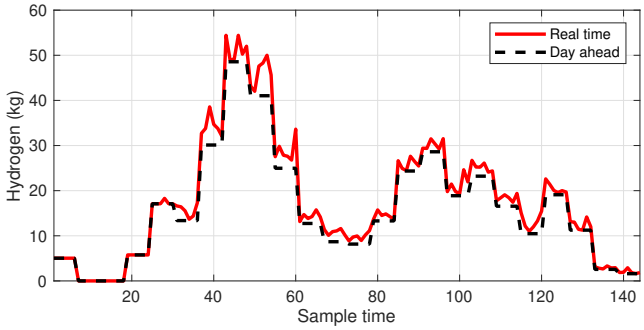

Figure 10: Output of the hydrogen tank

One part of the electricity purchased from the electricity market is entered to

the P2G to convert the electricity to natural gas. Fig. 12-a. The P2G consumes electricity during intra-hours 1-30 (1-5 in DA), where the electricity is purchased from the DA electricity market. The generated gas is discharged during hours 1-5 in the DA horizon, directly. Since the RM prices in Fig. 6 increases dramatically compared to the DA during intra-hours 1-30, the electricity procured for the P2G during the mentioned interval reduces to zero. For the interval 31-60, the P2G consumes electricity to lower prices of the electricity compared to the natural gas. Besides, the gas discharges only during the interval that the gas price is high.

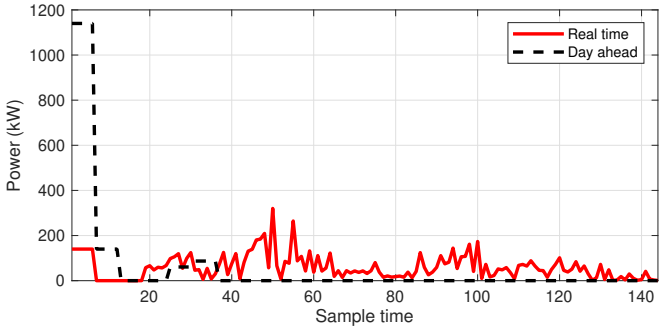

Figure 11: Electricity generated by the FC

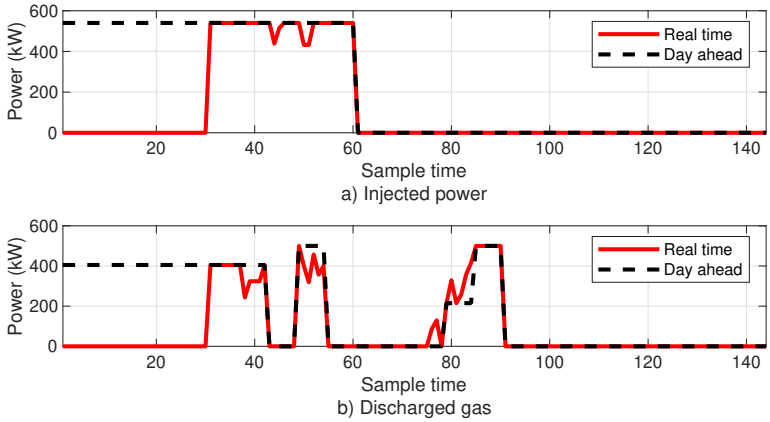

Figure 12: Electricity consumed by the P2G unit

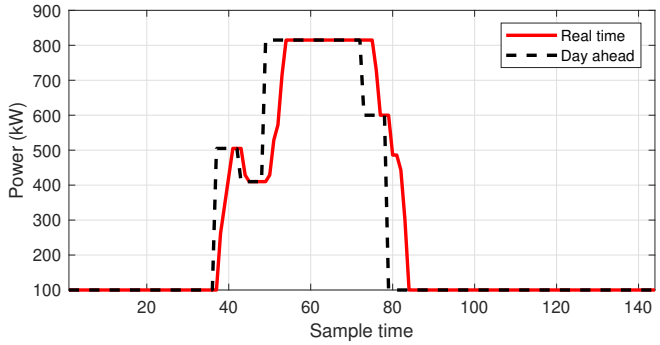

Figure 13: Level of natural gas in the gas storage system

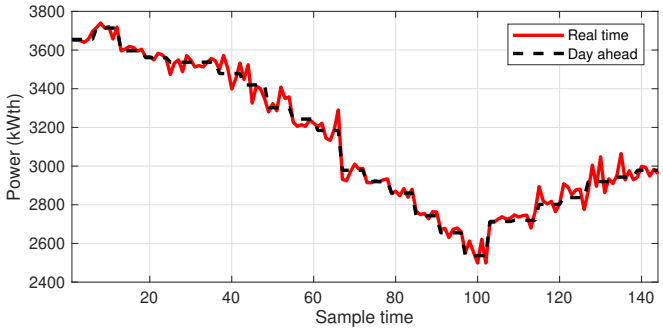

Figure 14: Heat generated by the boiler

Fig. 13 shows the gas storage state of charge, where the RT decisions follow the DA decisions properly, as the decision of the DA and RT are close in Fig. 12, exactly during the interval the gas storage level is higher than its minimum value. According to Fig. 14, all the errors of the heat demands are compensated by the boiler. While the CHP in Fig. 15 participates to support the electrical loads by its maximum value during the peak interval of the load demand and the minimum value of the feasible operation region for the rest of the interval. It always generates heat and electricity with minimum and maximum values. Note that it reduces its production again during 91-108, where the heat demands are at the off-peak.

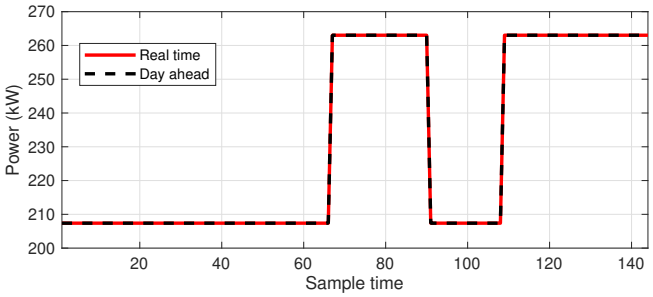

Figure 15: Output of the CHP unit

5.3. Complexity order

This subsection provides further elaboration on the complexity level of the formulated model. Computational dimensions of the proposed model, including the number of binary and continuous variables as well as the number of equality and inequality constraints for the case study presented in sub-section 5.1 are presented in Table 3. As it is obvious from the table, the problem's order of complexity is increased linearly by increasing the number of scenarios and the number of operating timeslots, and intra-hour operating timeslots. This can be considered as one of the advantages of the proposed linear model for this complex problem.

The developed model has been solved in GAMS using the CPLEX solver. The complete duration for the computation on a system that has 16 cores, a 3.6 GHz CPU, and 32 GigaBytes of RAM was recorded as 284.64 seconds.

Table 3: Computational complexity of the problem

Type of #	Order of complexity	Current size of the model
# of binary variables	$\|\mathcal{T}\| + 9\|\S\|\|\mathcal{T}\|\|\mathcal{T}_t\|$	12984
# of continuous variables	$3 + 4\|\mathcal{T}\|\|\mathcal{T}_t\| + 23\|\mathcal{T}\| + 37\|\S\|\|\mathcal{T}\|\|\mathcal{T}_t\| + 2\|\mathcal{T}\|\|\S\|$	54891
# of equality constraints	$3 + 10\|\mathcal{T}\| + 13\|\S\|\|\mathcal{T}\|\|\mathcal{T}_t\| + 3\|\mathcal{T}\|\|\S\| + 2\|\mathcal{T}_t\|\|\S\|$	19803
# of inequality constraints	$9\|\mathcal{T}\| + 55\|\S\|\|\mathcal{T}\|\|\mathcal{T}_t\| + 2\|\mathcal{T}\|\|\S\| + 4\|\mathcal{T}\|\|\mathcal{T}_t\|$	80472

6. Conclusions

In this paper, a hybrid stochastic-robust framework is presented for the optimal operation of a hydrogen-based energy hub to participate in day-ahead and regulation markets. The RO part considers the uncertainty of the electricity market prices in RM, while the uncertainty of the electricity and heat demands, the driving pattern of hydrogen vehicles, and the initial state of charge of the HVs are addressed by stochastic programming. The results demonstrate the following items:

- The decisions in the DA market change in RM by regulation up/down actions to compensate for the forecasting error of the DA electricity loads.
- The hydrogen tank is charged using the hydrogen released by the electrolyzer to refuel the HVs. The HT charges mostly during reasonable pricing hours.
- The existence of the HT resulted in proper refueling of the HVs in DA and compensating for the errors in the RT horizon.
- Due to the increase in the FC production to compensate for the RT demands error, the RT discharge of the HT is always higher than or equal to the DA values.
- The P2G is fed by electricity, when the electricity prices are lower than gas prices, while the decisions may change, paying attention to the difference of the RM and DA prices.
- The CHP participates to support the electrical loads by its maximum value during the peak interval of the load demand, while it respects the minimum values of the feasible operation region during the off-peak period of the demands.

A networked constrained framework for the operation of hydrogen refueling stations will be considered as the prospect of future work, where private hydrogen refueling stations interact actively with an active distribution network.

Acknowledgment

Omid Homaee and Arsalan Najafi would like to acknowledge the support by Polish National Agency for Academic Exchange for the grants No.BPN/ULM/2021/1/00227, and PPN/ULM/2020/1/00196, respectively.

References

[1] J. Zhou, S. Li, X. Zhou, C. Li, Z. Xiong, Y. Zhao, G. Liang, Operation optimization for gas-electric integrated energy system with hydrogen storage module, International Journal of Hydrogen Energy 47 (86) (2022) 36622–36639. doi:https://doi.org/10.1016/j.ijhydene.2022.08.224. URL https://www.sciencedirect.com/science/article/pii/S0360319922038344

[2] J. Wang, X. Sun, Y. Jiang, J. Wang, Assessment of a fuel cell based-hybrid energy system to generate and store electrical energy, Energy Reports 8 (2022) 2248–2261, cited By 0. doi:10.1016/j.egyr.2022.01.053.

[3] A. Najafi, M. Pourakbari-Kasmaei, M. Jasinski, M. Lehtonen, Z. Leonowicz, A max–min–max robust optimization model for multi-carrier energy systems integrated with power to gas storage system, Journal of Energy Storage 48 (2022) 103933. doi:https://doi.org/10.1016/j.est.2021.103933.

[4] A. Dini, A. Hassankashi, S. Pirouzi, M. Lehtonen, B. Arandian, A. A. Baziar, A flexible-reliable operation optimization model of the networked energy hubs with distributed generations, energy storage systems and demand response, Energy 239 (2022) 121923. doi:10.1016/j.energy.2021.121923.

[5] A. Ebrahimi-Moghadam, M. Farzaneh-Gord, Optimal operation of a multi-generation district energy hub based on electrical, heating, and cooling demands and hydrogen production, Applied Energy 309 (2022) 118453. doi:10.1016/j.apenergy.2021.118453.

[6] J. Wang, K. Xue, Y. Guo, J. Ma, X. Zhou, M. Liu, J. Yan, Multi-objective capacity programming and operation optimization of an integrated energy system considering hydrogen energy storage for collective energy communities, Energy Conversion and Management 268 (2022) 116057. doi:https://doi.org/10.1016/j.enconman.2022.116057.
URL https://www.sciencedirect.com/science/article/pii/S0196890422008457

[7] Q. Wu, C. Li, Economy-environment-energy benefit analysis for green hydrogen based integrated energy system operation under carbon trading with a robust optimization model, Journal of Energy Storage 55 (2022) 105560. doi:https://doi.org/10.1016/j.est.2022.105560.
URL https://www.sciencedirect.com/science/article/pii/S2352152X22015511

[8] S. M. Tatar, H. Akulker, H. Sildir, E. Aydin, Optimal design and operation of integrated microgrids under intermittent renewable energy sources coupled with green hydrogen and demand scenarios, International Journal of Hydrogen Energy 47 (65) (2022) 27848–27865. doi:https://doi.org/10.1016/j.ijhydene.2022.06.130.
URL https://www.sciencedirect.com/science/article/pii/S0360319922027628

[9] M. Nasir, A. Rezaee Jordehi, S. A. A. Matin, V. S. Tabar, M. Tostado-Véliz, S. A. Mansouri, Optimal operation of energy hubs including parking lots for hydrogen vehicles and responsive demands, Journal of Energy Storage 50 (2022) 104630. doi:https://doi.org/10.1016/j.est.2022.104630.
URL https://www.sciencedirect.com/science/article/pii/S2352152X22006454

[10] M. Agabalaye-Rahvar, A. Mansour-Saatloo, M. Mirzaei, B. Mohammadi-Ivatloo, K. Zare, Economic-environmental stochastic scheduling for hydrogen storage-based smart energy hub coordinated with

integrated demand response program, International Journal of Energy Research 45 (14) (2021) 20232–20257, cited By 2. doi:10.1002/er.7108.
URL https://www.scopus.com/inward/record.uri?eid=2-s2.0-85112201345&doi=10.1002%2fer.7108&partnerID=40&md5=cdec7ecd0f429db6da99c343795b4343

[11] C. Thommessen, M. Otto, F. Nigbur, J. Roes, A. Heinzel, Techno-economic system analysis of an offshore energy hub with an outlook on electrofuel applications, Smart Energy 3, cited By 5 (2021). doi:10.1016/j.segy.2021.100027.
URL https://www.scopus.com/inward/record.uri?eid=2-s2.0-85115752757&doi=10.1016%2fj.segy.2021.100027&partnerID=40&md5=fbaeecef6494537de4e9a50d55261d8f

[12] P. Zhao, C. Gu, Z. Cao, Z. Hu, X. Zhang, X. Chen, I. Hernando-Gil, Y. Ding, Economic-effective multi-energy management considering voltage regulation networked with energy hubs, IEEE Transactions on Power Systems 36 (3) (2021) 2503–2515. doi:10.1109/TPWRS.2020.3025861.

[13] Z. Yuan, S. He, A. Alizadeh, S. Nojavan, K. Jermsittiparsert, Probabilistic scheduling of power-to-gas storage system in renewable energy hub integrated with demand response program, Journal of Energy Storage 29, cited By 37 (2020). doi:10.1016/j.est.2020.101393.
URL https://www.scopus.com/inward/record.uri?eid=2-s2.0-85082961973&doi=10.1016%2fj.est.2020.101393&partnerID=40&md5=b2d6ca3c7e01bfa1f874aaa561a6a838

[14] S. Geng, M. Vrakopoulou, I. A. Hiskens, Optimal capacity design and operation of energy hub systems, Proceedings of the IEEE 108 (9) (2020) 1475–1495.

[15] A. Mansour-Saatloo, M. Agabalaye-Rahvar, M. A. Mirzaei, B. Mohammadi-Ivatloo, M. Abapour, K. Zare, Robust scheduling of hydrogen based smart micro energy hub with integrated demand

response, Journal of Cleaner Production 267 (2020) 122041. doi:https://doi.org/10.1016/j.jclepro.2020.122041.
URL https://www.sciencedirect.com/science/article/pii/S0959652620320886

[16] X. Wei, X. Zhang, Y. Sun, J. Qiu, Carbon emission flow oriented tri-level planning of integrated electricity-hydrogen-gas system with hydrogen vehicles, IEEE Transactions on Industry ApplicationsCited By 1 (2021). doi:10.1109/TIA.2021.3095246.

[17] S. Klyapovskiy, Y. Zheng, S. You, H. W. Bindner, Optimal operation of the hydrogen-based energy management system with p2x demand response and ammonia plant, Applied Energy 304 (2021) 117559. doi:https://doi.org/10.1016/j.apenergy.2021.117559.
URL https://www.sciencedirect.com/science/article/pii/S0306261921009375

[18] X. Wu, H. Li, X. Wang, W. Zhao, Cooperative operation for wind turbines and hydrogen fueling stations with on-site hydrogen production, IEEE Transactions on Sustainable Energy 11 (4) (2020) 2775–2789. doi:10.1109/TSTE.2020.2975609.

[19] C. Shao, C. Feng, M. Shahidehpour, Q. Zhou, X. Wang, X. Wang, Optimal stochastic operation of integrated electric power and renewable energy with vehicle-based hydrogen energy system, IEEE Transactions on Power Systems 36 (5) (2021) 4310–4321. doi:10.1109/TPWRS.2021.3058561.

[20] A. Najafi, M. Pourakbari-Kasmaei, M. Jasinski, M. Lehtonen, Z. Leonowicz, A hybrid decentralized stochastic-robust model for optimal coordination of electric vehicle aggregator and energy hub entities, Applied Energy 304 (2021) 117708.

[21] A. Mansour-Saatloo, M. A. Mirzaei, B. Mohammadi-Ivatloo, K. Zare, A risk-averse hybrid approach for optimal participation of power-to-hydrogen

technology-based multi-energy microgrid in multi-energy markets, Sustainable Cities and Society 63 (2020) 102421.

[22] N. Nasiri, S. Zeynali, S. N. Ravadanegh, M. Marzband, A hybrid robust-stochastic approach for strategic scheduling of a multi-energy system as a price-maker player in day-ahead wholesale market, Energy 235 (2021) 121398.

[23] Q. Guo, S. Nojavan, S. Lei, X. Liang, Economic-environmental evaluation of industrial energy parks integrated with cchp units under a hybrid igdt-stochastic optimization approach, Journal of Cleaner Production 317 (2021) 128364. doi:https://doi.org/10.1016/j.jclepro.2021.128364.
URL https://www.sciencedirect.com/science/article/pii/S0959652621025774

[24] A. Najafi, M. Pourakbari-Kasmaei, M. Jasinski, M. Lehtonen, Z. Leonowicz, A medium-term hybrid igdt-robust optimization model for optimal self scheduling of multi-carrier energy systems, Energy 238 (2022) 121661. doi:https://doi.org/10.1016/j.energy.2021.121661.
URL https://www.sciencedirect.com/science/article/pii/S0360544221019095

[25] A. Mansour-Satloo, M. Agabalaye-Rahvar, M. A. Mirazaei, B. Mohammadi-Ivatloo, K. Zare, A. Anvari-Moghaddam, A hybrid robust-stochastic approach for optimal scheduling of interconnected hydrogen-based energy hubs, IET Smart Grid 4 (2) (2021) 241–254. doi:10.1049/stg2.12035.

[26] A. Najafi, A. Tavakoli, M. Pourakbari-Kasmaei, M. Lehtonen, A risk-based optimal self-scheduling of smart energy hub in the day-ahead and regulation markets, Journal of Cleaner Production 279 (2021) 123631. doi:https://doi.org/10.1016/j.jclepro.2020.123631.
URL https://www.sciencedirect.com/science/article/pii/S0959652620336763

[27] W. Sun, G. P. Harrison, Active load management of hydrogen refuelling stations for increasing the grid integration of renewable generation, IEEE Access 9 (2021) 101681–101694. doi:10.1109/ACCESS.2021.3098161.

[28] Y. Xiao, X. Wang, P. Pinson, X. Wang, A local energy market for electricity and hydrogen, IEEE Transactions on Power Systems 33 (4) (2018) 3898–3908. doi:10.1109/TPWRS.2017.2779540.

[29] X. Wu, S. Qi, Z. Wang, C. Duan, X. Wang, F. Li, Optimal scheduling for microgrids with hydrogen fueling stations considering uncertainty using data-driven approach, Applied Energy 253 (2019) 113568. doi:https://doi.org/10.1016/j.apenergy.2019.113568.
URL https://www.sciencedirect.com/science/article/pii/S0306261919312425

[30] X. Wu, H. Li, X. Wang, W. Zhao, Cooperative operation for wind turbines and hydrogen fueling stations with on-site hydrogen production, IEEE Transactions on Sustainable Energy 11 (4) (2020) 2775–2789. doi:10.1109/TSTE.2020.2975609.

[31] X. Wu, W. Zhao, H. Li, B. Liu, Z. Zhang, X. Wang, Multi-stage stochastic programming based offering strategy for hydrogen fueling station in joint energy, reserve markets, Renewable Energy 180 (2021) 605–615. doi:https://doi.org/10.1016/j.renene.2021.08.076.
URL https://www.sciencedirect.com/science/article/pii/S0960148121012428

[32] Q. Zeng, J. Fang, J. Li, Z. Chen, Steady-state analysis of the integrated natural gas and electric power system with bi-directional energy conversion, Applied Energy 184 (2016) 1483–1492. doi:10.1016/j.apenergy.2016.05.060.
URL https://www.sciencedirect.com/science/article/pii/S0306261916306572

[33] A. Najafi, H. Falaghi, J. Contreras, M. Ramezani, Medium-term energy hub management subject to electricity price and wind uncertainty, Applied Energy 168 (2016) 418–33.

[34] H. Khani, N. A. El-Taweel, H. E. Z. Farag, Supervisory scheduling of storage-based hydrogen fueling stations for transportation sector and distributed operating reserve in electricity markets, IEEE Transactions on Industrial Informatics 16 (3) (2020) 1529–1538. doi:10.1109/TII.2019.2926779.